1974

A Design Report on a Servo Controlled Inertial Sensor Test Fixture

James B. Dowdle
University of Central Florida

A DESIGN REPORT ON A SERVO CONTROLLED INERTIAL SENSOR TEST FIXTURE

BY

JAMES B. DOWDLE, JR.
B.S., University of Miami, 1972

RESEARCH REPORT

Submitted in partial fulfillment of the requirements
for the degree of Master of Science in Engineering
in the Graduate Studies Program of
Florida Technological University

Orlando, Florida
1974

ABSTRACT

A DESIGN REPORT ON A SERVO CONTROLLED
INERTIAL SENSOR TEST FIXTURE
by
James B. Dowdle, Jr.

This report discusses the design of a servo controlled positioning system for remote control positioning of inertial sensors while under high acceleration test in a centrifuge.

A rotating fixture and an electronic control panel was built for this purpose, with two modes of operation. The fixture can be positioned with an accuracy of 0.05 degrees and a resolution of 0.01 degrees, or it can be maintained in a constant velocity mode at rates from 1 to 16 degrees per second.

The velocity loop was implemented as a phase locked loop, and the command rate is entered as a frequency - from a function generator or a frequency synthesizer. The position loop employs a pick-off resolver for sensing position and a control resolver for entering the command position.

The paper presents the entire design picture, including a consideration of design alternatives, and servo and electronic circuit design. Photographs of the system in operation are shown in the appendix.

Approved: Fred C. Simons, Jr.
Director of Research Report

FORWARD

The topic of this paper will be the design of an electro-mechanical servo control system for remote positioning of inertial sensors while under a high acceleration environment in a centrifuge. The system was designed and built by the Inertial Sensors Group of Martin Marietta Aerospace at Orlando, Florida. The servo analysis and the electronic circuit design for the system was done by James B. Dowdle, Jr., and will compose the body of this paper.

Also included will be some discussion of the performance of the completed system, including photos of equipment and oscilloscope traces at various points in the circuitry.

CONTENTS

LIST OF ILLUSTRATIONS

LIST OF ILLUSTRATIONS (Continued)

CHAPTER I

INTRODUCTION

Due to the high acceleration capability and reliability required of some modern inertial guidance packages, the inertial sensors themselves are exposed to and operated under high-g environments. A steady-state acceleration may be imposed upon a sensor by placing it in a large centriguge, and adjusting the distance from the center of rotation, and the rate of rotation to obtain the desired acceleration level. With such a system, it is desirable to be able to turn the sensor orientation with respect to the acceleration vector without having to stop and open the centrifuge, and manually reposition the sensor. A remote positionable fixture saves a great deal of time, as well as adding new test capability to the system.

It was decided to build such a fixture, capable of holding a number of types of sensors. It would have a drive motor and position sensing devices for remote control positioning of the test orientation. An electronic control panel was built, which received positional information and transmitted command signals through a network of slip rings in the centrifuge and in the fixture itself. The purpose of the control panel was to operate the fixture in two modes: One, allowing the test sample to be positioned in any desired angular orientation in the horizontal plane, and the other allowing the sample to be rotated at a constant angular velocity in the same plane, with rates continuously selectable over a range from 6 to 12 degrees per second.

Thus, the objective of the following chapters will be to present material pertinent to the design of both the position and the velocity control loops of the above mentioned system.

CHAPTER II

DEFINING THE DESIGN PROBLEM

Once the design objectives are clear, there are probably many ways in which the problem may be solved. Therefore, some time must be spent in evaluating various approaches to the problem before a large amount of work is done on the detailed analysis and design.

The objective of this design will be to produce a control system capable of operating in two modes: velocity and position. In the velocity mode, it will be desirable to have a system which will hold the angular rate constant, that is, non-varying with changing load. Since the system will be used with data recording equipment which records simultaneously angular position of the fixture turntable and sensor parameters which may vary with angular position, the frequency response of the velocity loop should be such that the fixture rate will not significantly lag the command signal as the fixture turntable rotates at the design speeds from 6 to 12 degrees per second.

The position loop will be used for various test purposes, requiring varying degrees of accuracy. The loop should be designed, however, to enable the turntable position to be adjusted with a resolution of at least the accuracy of the position readout equipment.

Now consider what there is to work with. A drive motor and gear train has already been chosen. In selecting the drive, the primary consideration was in finding a motor capable of putting out sufficient torque to overcome the large mass unbalance torques which

will be encountered under a high-g. environment. The drive assembly was ordered complete with the motor, the gear train, a tachometer, and the power amplifier to drive the motor. The drive is capable of delivering output rates from -12 to +12 degrees per second with 285 inch-pounds of torque at the maximum rate, and 415 inch-pounds at zero rate.

The position readout also has been chosen. The instrument is a digital synchro/resolver angle indicator. It requires a synchro or resolver input, and provides both an LED digital readout and BCD angular outputs. (i.e., 0.01^{o}, 0.02^{o}, 0.04^{o}, ..., 80^{o}, 100^{o}, 200^{o}) The instrument is basically an analog to digital converter, and has an accuracy of 0.03^{o} and a resolution of 0.01^{o}. The BCD outputs change continuously with resolver (or synchro) position.

A two phase resolver was chosen to drive the angle indicator, and the accuracy of this resolver is 0.05^{o}. This resolver is mounted on the fixture, and senses the angle of the fixture turntable which is in turn displayed digitally upon the angle indicator.

For position commands, another resolver was chosen which could be mounted to a control knob. The control has both a course and fine adjustment, with the course being marked in graduations of one degree, and the fine having a resolution of one-quarter degree per turn.

Let us now consider how a position control loop might be built. As shown in Figure 2.1, the turntable has one phase of the rotor shorted, while the other phase is energized with 26 volts at 400 cycles per second. With this arrangement, the stator phases provide two voltage sources in quadrature which together define the rotor position.

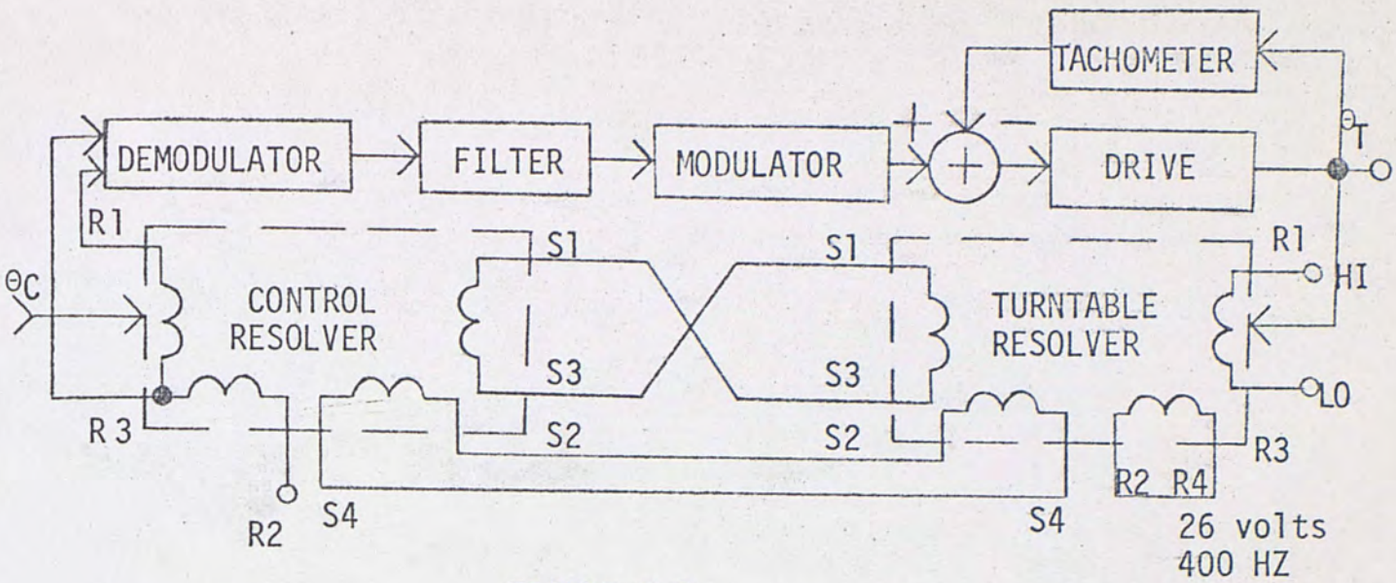

FIGURE 2.1

THE POSITION CONTROL LOOP

These two stator voltages are then used to energize the control resolver by connecting the stators of both resolvers in parallel. Then, the voltages appearing across the two rotor windings of the control resolver will be in quadrature, and will be double side-band suppressed carrier modulated by rotation of the turntable. Each rotor winding will have two in phase fundamental noll outputs as the turntable rotates through one revolution, and one of these phases may be used to drive the servo amplifier. The positions of the turn-table at which the nulls occur may be selected by rotating the control resolver to the desired setting. The null will be caused to occur by the servo electronics, which will drive the turntable to the point at which the null occurs. Only one of the two null positions will be sought out, as determined by the phasing of the control loop.

The error voltage coming from winding R1 - R3 of the control resolver in Figure 1 will be 400 Hz, with a peak level of 26 volts RMS. In order

to adjust the bandwidth of the system and to apply compensating techniques, it will be necessary to convert the error voltage to the DC domain. The demodulator shown is a coherent demodulator synchronized to the 26 volt, 400 Hz resolver source which is the reference for the entire system. Once the error voltage is converted to D.C., it may be operated upon effectively and the 400 Hz ripple may be removed.

The drive motor and the tachometer operate on 400 Hz which means it will be n ecessary to modulate the output of the filter. The modulator shown is a double sideband suppressed carrier modulator, synchronized to the 400 Hz source. Back in the A.C. domain, the tachometer output is summed with the output of the modulator and the result is applied to the input of the drive stage. The tachometer is required to control system transient behavior.

To configure a block diagram for the velocity control loop, further consideration is required. One approach is to sum a command voltage against the tachometer output to produce an error voltage to drive the turntable at the desired rate. However, tachometers lack the required accuracy and are noisy.

As a matter of fact, this is one of the reasons why the angle indicator was purchased. As has been said earlier, the indicator has BCD outputs which change state continuously as the input resolver senses rotation. That is, these outputs will change state at a rate proportional to the rate of rotation of the turntable, so, the 0.01 degree output, for example, will be a symmetrical square wave frequency modulated by the rate

of turntable rotation. This property allows the angle indicator to be used as an extremely accurate rate encoder.

Once this was realized, two methods for utilizing this asset of the angle indicator were considered. The first approach taken was to demodulate the 0.01 degree output using circuitry which operates on the principle of period measuring for FM demodulation. The second thought was to digitally detect the information contained in the 0.01 degree output, and to enter rate commands by means of a frequency synthesizer (a function generator for less demanding applications). In considering how such circuitry might be implemented, it became apparent that such a system would best be implemented as a phase-locked loop.

Figure 2.2 shows how the angle indicator may be used as the feedback element, and a square wave generator as the control element in a phase-locked velocity control system. The feedback wave form will generate

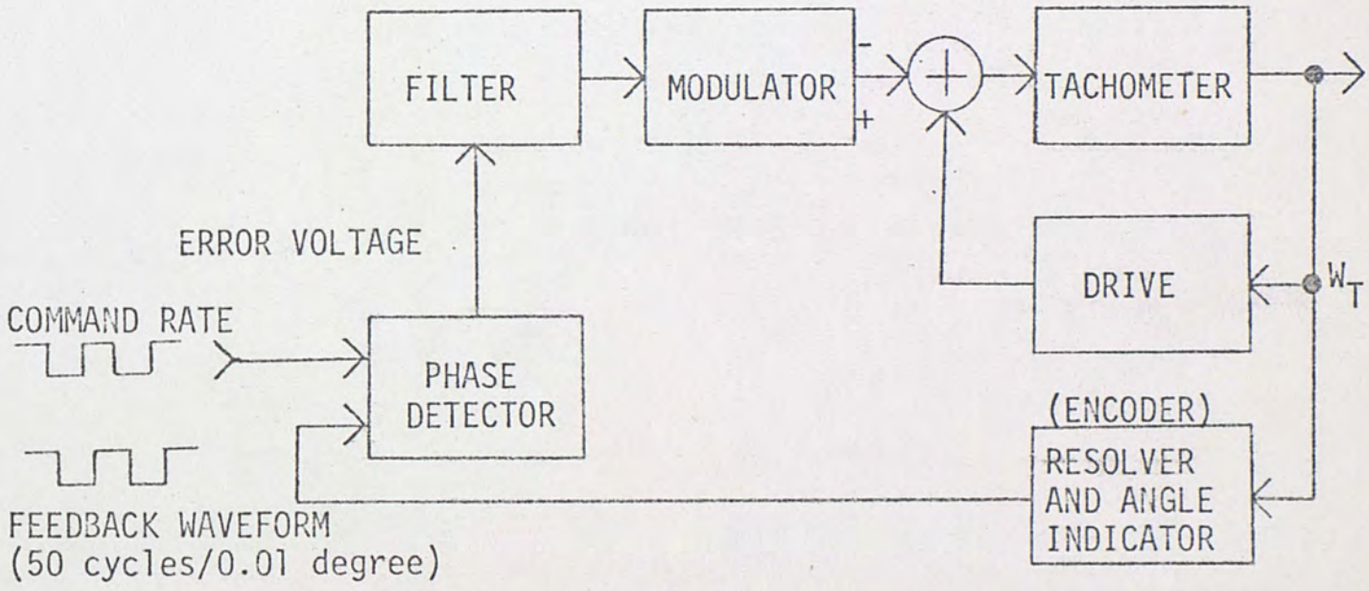

FIGURE 2.2

PHASE-LOCKED VELOCITY CONTROL LOOP

50 cycles per 0.01 degree, so the gain of the angle indicator used as an encoder will be as follows:

$$K_E = 50 \frac{\text{cycles}}{\text{degree}} \times 360 \frac{\text{degrees}}{\text{revolution}}$$

$$K_E = 18{,}000 \frac{\text{cycles}}{\text{revolution}}$$

The phase detector is digital in nature and its output is a series of pulses whose area is proportional to phase error between the command frequency and the feedback frequency. The output pulse train is periodic with a frequency equal to the command frequency, and thus requires filtering. The remainder of the loop is as in Figure 1.

The phase-locked technique provides a significant advantage over the other methods considered in that an extremely accurate command source - such as a frequency synthesizer - may be used, and the turntable velocity will follow, locked in phase, with zero steady state velocity error, when the loop is locked. Moreover, a standard chip was discovered which would serve as the phase detector, making the circuitry for the phase-locked technique much simpler than that of period measuring demodulation, and the phase-locked technique was chosen.

Now that the format of the design for the two loops has been determined, the details of the design may be explored. The following chapters will deal with the servo analysis of the two loops, and the associated circuit design.

CHAPTER III

THE DESIGN OF THE VELOCITY SERVO LOOP

As the velocity servo loop portion of the design is probably more dominate over the format and makeup of the entire system than is the position loop, the design of the velocity servo loop will be considered first. As shown in Figure 2.2, the loop is to operate as a phase-locked loop, and the functional blocks which will be required have been defined. The procedure now will be to define the transfer function of each block, so that the closed loop transfer function may be determined. Once this has been done, the loop variables may be chosen to fulfill the design requirements.

Let us start with the block in Figure 2.2 which is labeled "drive". This block consists of the motor power amplifier, the motor, and the turntable. As shown in Figure 3.1, a low level 400 cycle per second error voltage is applied to the power amplifier inputs, and the output

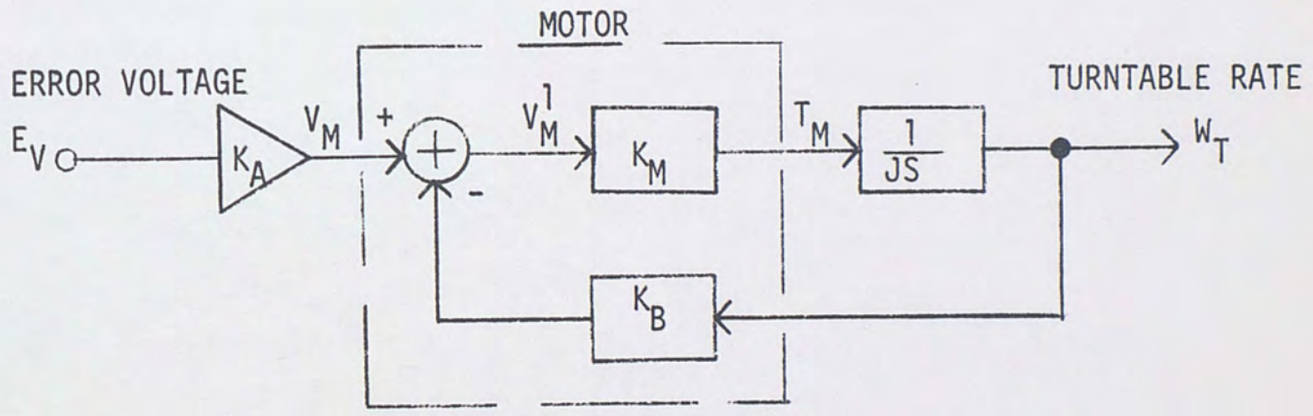

FIGURE 3.1
DRIVE DYNAMIC MODEL

of the amplifier is applied directly to the motor. The model as shown accounts for the zero speed scale factor of the motor (K_m), and the back EMF and viscous friction coefficient of the motor (K_B). The output of the motor is a torque, which when divided by the inertia of the turntable (J) yields an angular acceleration of the turntable. The "1/S" term integrates accelerations to yield angular rate, the desired output. The transfer function of this entire loop may be derived as follows:

$$G(S) = \frac{W_T}{V_M^1} = \frac{K_M}{JS} \quad , \quad H(S) = K_B$$

$$T^1(S) = \frac{G(S)}{1+G(S)\ H(S)} = \frac{W_T}{V_M} = \frac{K_M/JS}{1+K_B\ K_M/JS}$$

$$T^1(S) = \frac{W_T}{V_M} = \frac{K_M/J}{S + K_B\ K_M/J}$$

$$T(S) = K_A\ T^1(S)$$

$$T(S) = \frac{K_A\ K_M/J}{S+K_B \cdot K_M/J} \qquad (3.1)$$

Now, let us add to the model the tachometer feedback block as shown in Figure 2.2, and call the resulting block "turntable drive", as shown in Figure 3.2 below.

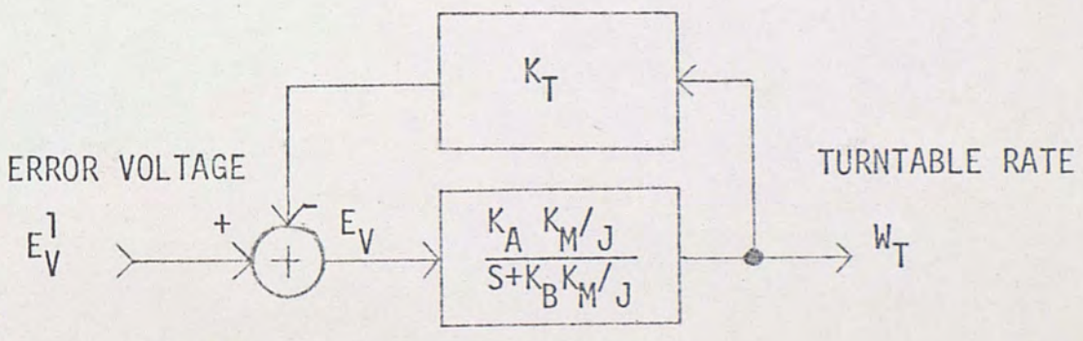

FIGURE 3.2 - TURNTABLE DRIVE

The transfer function of the new "turntable drive" block may be derived as follows:

$$G(S) = \frac{W_T}{E_V} = \frac{K_A \; K_M \; /J}{S+K_B \; K_M/J}$$

$$H(S) = K_T$$

$$T(S) = \frac{G(S)}{1+G(S)H(S)} = \frac{K_A \; K_M/J}{S+\frac{K_B \; K_M}{J} + \frac{K_A K_M K_T}{J}}$$

$$T(S) = \frac{\frac{W_T}{E_V}}{1} = \frac{K_A K_M/J}{S+\frac{K_M(K_B+K_A K_T)}{J}} \qquad (3.2)$$

Consider now the "encoder" block of Figure 2.2. As has been said in Chapter 2, it was decided to use the 0.01 degree output as the encoder for the feedback of the velocity loop. The 0.01 degree output will be a square wave as illustrated in Figure 3.3, and there will be 50 cycles of the square wave in 1.00 degree of rotation.

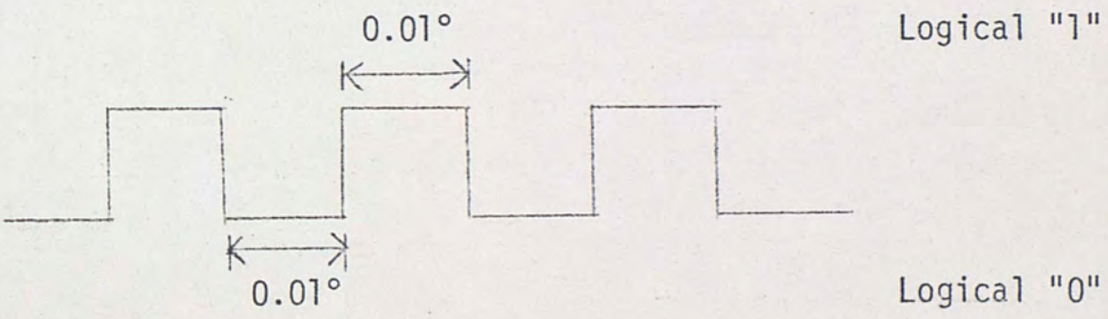

FIGURE 3.3

0.01 DEGREE OUTPUT OF ANGLE INDICATOR
WITH CONSTANT RATE INPUT

Therefore, the scale factor of the encoder may be determined as follows:

$$K_E = 50\left(\frac{\text{cycles}}{\text{degree}}\right) \times 360\left(\frac{\text{degrees}}{\text{revolution}}\right)$$

$$K_E = 18{,}000\left(\frac{\text{cycles}}{\text{revolution}}\right) \qquad (3.3)$$

Now consider the "phase dector" block of the velocity servo. When the system is phase-locked, the gain of block is K_ϕ (VDC/RADIAN). Also, since the detector yields an error voltage proportional to phase (or position) error - and since the two inputs to the detector are rates - there is a "1/S" term implied in the block in order to convert rate error to position error. The phase detector may be modeled as shown in Figure 3.4 below.

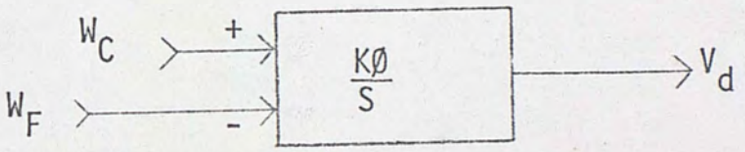

FIGURE 3.4

PHASE DETECTOR MODEL

the transfer function for this block is simply as follows:

$$T(S) = \frac{V_d}{W_C - W_F} = \frac{K_\phi}{S} \qquad (3.4)$$

The "modulator" block of the velocity loop is simply a DC to AC converter, the DC being the output of the "filter" block, and the AC being the 400 Hz. AC signal which is required to drive the motor power amplifier. The modulator gain is simply K_{CN} (VAC/VDC).

The "filter" block of Figure 2.2 is the heart of the closed loop system in that its makeup will determine the passband of the loop, steady-state performance, and the stability of the system. This block is best understood as two sub-blocks: 1) the loop filter; and 2) the integrator/compensator block.

The loop filter was chosen to be a second order Butterworth, since, as will be seen later, this will result in a closed loop transfer function which has a denominator which is fourth order Butterworth.

The break frequency of the fourth order denominator polynomial was chosen to be 20 cycles per second, because this will result in more than adequate system frequency response, and will roll off at a rate of 80dB per decade to provide adequate filtering of the pulse train output of the phase detector. The phase detector will put out a pulse train of frequency W_C, and the DC level of the pulse train will provide the output: $V_d = \frac{K_\phi}{S} (W_C - W_F)$. Since the lowest rate of rotation will be 6 degrees per second, the command frequency (W_C) will be as follows.

$$W_C = K_E \cdot W_T$$

$$W_T = 6 \frac{(\text{Deg.})}{(\text{Sec})} \cdot \frac{1}{360} \frac{(\text{Cycles})}{(\text{Deg.})}$$

$$W_C = (18{,}000 \cdot 6)/360$$

$$W_C = 300 \frac{(\text{Cycles})}{(\text{Second})}$$

Therefore, at the lowest rate of rotation (worst case condition) the ripple will be suppressed by approximately 80dB. The loop filter parameters are shown in Figure 3.5 below. The constants α_1 and α_2 determine the damping and break frequency of the filter, and K_V is a gain constant associated with the circuitry required for the implementation of the filter. The meaning of these constants will be explained further in the design chapters of this paper.

The integrator/compensator block of the loop shown in Figure 3.5 serves to drive the steady-state position error to zero by the use of an integrator in the open loop transfer function (G[S]). As will be seen later as the closed loop transfer function is derived, the term $S+\frac{1}{T_1}$ is required in order to obtain fourth order Butterworth poles in the closed loop transfer function. The term $S+\frac{1}{T_3}$ is used to compensate for

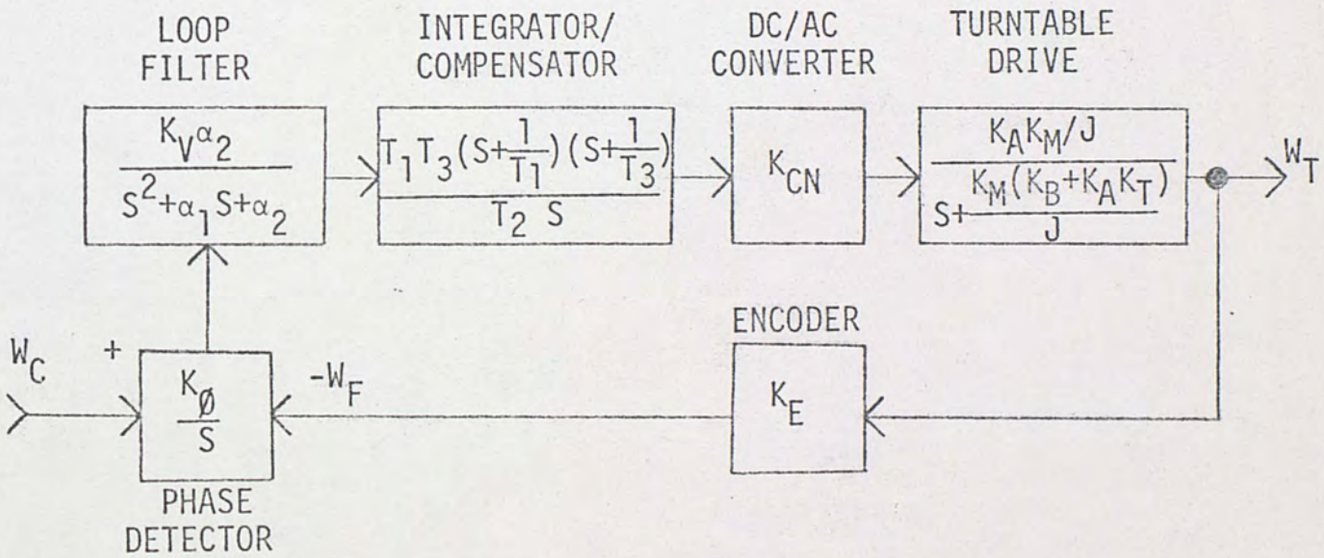

FIGURE 3.5

THE VELOCITY SERVO LOOP DYNAMICS

the lag in response of the motor. T_3 is chosen such that:

$$S + \frac{1}{T_3} = S + \frac{K_M(K_B+K_A K_T)}{J}$$

or

$$T_3 = \frac{J}{K_M(K_B+K_A K_T)} \qquad (3.5)$$

In this way, the motor lag will be canceled out by the circuitry lead. It is realized that the cancelation will be imperfect, but system response should be little effected since the break point of the motor response (with tachometer feedback) is far higher than the break frequency of the closed loop.

Refering to Figure 3.5, the closed loop transfer function (T[S]) may be determined easily as follows:

$$G(S) = \frac{K_\phi T_1 T_3 K_V \alpha_2 K_{CN} K_A K_M}{J T_2 S^2} \quad \frac{S + 1/T_1}{S^2+\alpha_1 S+\alpha_2} \qquad (3.6)$$

$$H(S) = K_E \qquad (3.7)$$

For convenience, let:

$$K_{OL} = \frac{K_\phi T_1 T_3 K_V \alpha_2 K_{CN} K_A K_M}{J T_2} \qquad (3.8)$$

and $$K_{CL} = K_E K_{OL} \qquad (3.9)$$

$$T(S) = \frac{K_{OL}(S+1/T_1)}{S^4 + \alpha_1 S^3 + \alpha_2 S^2 + K_{CL} S + \frac{K_{CL}}{T_1}} \qquad (3.10)$$

Note that in equation (3.6), it has been assumed that $(S+\frac{1}{T_3})$ and $(S+\frac{K_M(K_B+K_AK_T)}{J})$ have canceled out.

Equation (3.10) is the closed loop transfer function of the velocity loop. The denominator is fourth order, and there is a first order break in the numerator. If we choose the constants in (3.10) such that the denominator polynomial is fourth order Butterworth, the roots will of course lie in the left half plane - implying stability - and the system performance will be predictable.

The normalized fourth order Butterworth polynomial is as given in equation (3.11). If the break frequency of this polynomial is chosen to be 20 cycles per second - as explained earlier in this chapter - then the polynomial may be denormalized as shown below, yielding the required values for the system constants.

Normalized fourth order Butterworth polynomial: [1]

$$S^4 + 2.613\ S^3 + 3.414\ S^2 + 2.613\ S + 1 \qquad (3.11)$$

$$f_B = 20\ \text{Hz} \rightarrow W_B = 2\pi.20 = 125.60\ \frac{(\text{RAD})}{(\text{Sec})}$$

The denormalized Butterworth polynomial is:

$$S^4 + 3.284\cdot10^2 S^3 + 5.391\cdot10^4 S^2 + 5.185\cdot10^6 S + 2.494.10^8 \qquad (3.12)$$

Equating coefficients of equation (3.12) with those of the denominator of equation (3.10), the following solutions are obtained:

$$\alpha_1 = 3.284\cdot10^2\ (1/\text{Sec}) \qquad (3.13)$$

$$\alpha_2 = 5.391\cdot10^4\ (1/\text{Sec}^2) \qquad (3.14)$$

[1] Mohammed Shusib Ghausi, Principles and Design of Linear Active Circuits (New York: MCGraw-Hill, Inc., 1965), p. 80.

$$K_{CL} = 5.185 \cdot 10^{6} (RAD/RAD) \tag{3.15}$$

$$T_1 = 2.079 \cdot 10^{-2} \ (Sec) \tag{3.16}$$

(3.3) and (3.9) yield:

$$K_{OL} = 2.881 \cdot 10^{2} (RAD/RAD) \tag{3.17}$$

We now need to consider equations (3.5) and (3.8), repeated here for convenience

$$T_3 = \frac{J}{K_M(K_B + K_A K_T)} \tag{3.5}$$

$$K_{OL} = \frac{K_\phi T_1 T_3 K_V \alpha_2 K_{CN} K_A K_M}{J T_2} \tag{3.8}$$

We now need to fill in the given constants in these two equations, in order to choose the remainder to meet the design goals. The following constants are known from motor and drive specifications, fixed circuit gains, etc.

$$K_\phi = 0.1194 \ (VDC/RAD) \tag{3.18}$$

$$K_A = 1500 \ (VAC/VAC) \tag{3.19}$$

$$K_T = 9.5113 \frac{(VAC)}{(RAD/SEC)} \tag{3.20}$$

$$K_M = 11.54 \ (IN\text{-}LB/VAC) \tag{3.21}$$

$$K_B = 53.11 \ \frac{(VAC)}{(RAD/SEC)} \tag{3.22}$$

$$J = 37.41 \ (IN\text{-}LB\text{-}SEC^2) \tag{3.23}$$

Substituting the appropriate gains above into equation (3.5), we obtain the following:

$$T_3 = \frac{37.41}{11.54(53.11 + 1500 \cdot 9.5113)}$$

$$T_3 = 2.264.10^{-4} \ (SEC) \tag{3.24}$$

Next, substituting equations (3.14), (3.16), (3.17), and (3.24), and the appropriate gains above into equation (3.8), the following is obtained:

$$K_{OL}=2.881\cdot 10^{2}=\frac{(.12)(2.08\cdot 10^{-2})(2.26\cdot 10^{-4})(K_V)(5.4\cdot 10^{4})K_{CN}(1500)(11.5)}{(37.41)T_2}$$

Therefore:

$$\frac{K_V K_{CN}}{T_2} = 2.055\cdot 10^{1} \qquad (3.25)$$

K_{CN} and T_2 were chosen for reasons associated with the electronic design - which will be covered in a later chapter - and therefore (3.25) may be further broken down to yield:

$$K_{CN} = 0.5\ \frac{(VAC)}{(VDC)} \qquad (3.26)$$

$$T_2 = 2.150\cdot 10^{-1}\ (SEC) \qquad (3.27)$$

$$K_V = 8.837\ \frac{(VOLTS)}{(VOLT\ )} \qquad (3.28)$$

We are now in a position to substitute the above constants into equations (3.6), (3.7), and (3.10) to obtain numerical solution for G(S), H(S), and T(S).

$$G(S) = \frac{2.881\cdot 10^{2}(S+4.809\cdot 10^{1})}{S^{2}(S^{2}+3.284\cdot 10^{2}S+5.391\cdot 10^{4})} \qquad (3.29)$$

$$H(S) = 18000 \qquad (3.30)$$

$$T(S) = \frac{2.88\cdot 10^{2}(S+4.809\cdot 10^{1})}{S^{4}+3.284\cdot 10^{2}S^{3}+5.391\cdot 10^{4}S^{2}+5.185\cdot 10^{6}S+2.494\cdot 10^{8}}$$

Figure 3.6 shows the velocity control loop, the closed loop transfer function, and the tabulated loop constants.

FIXTURE VELOCITY CONTROL LOOP

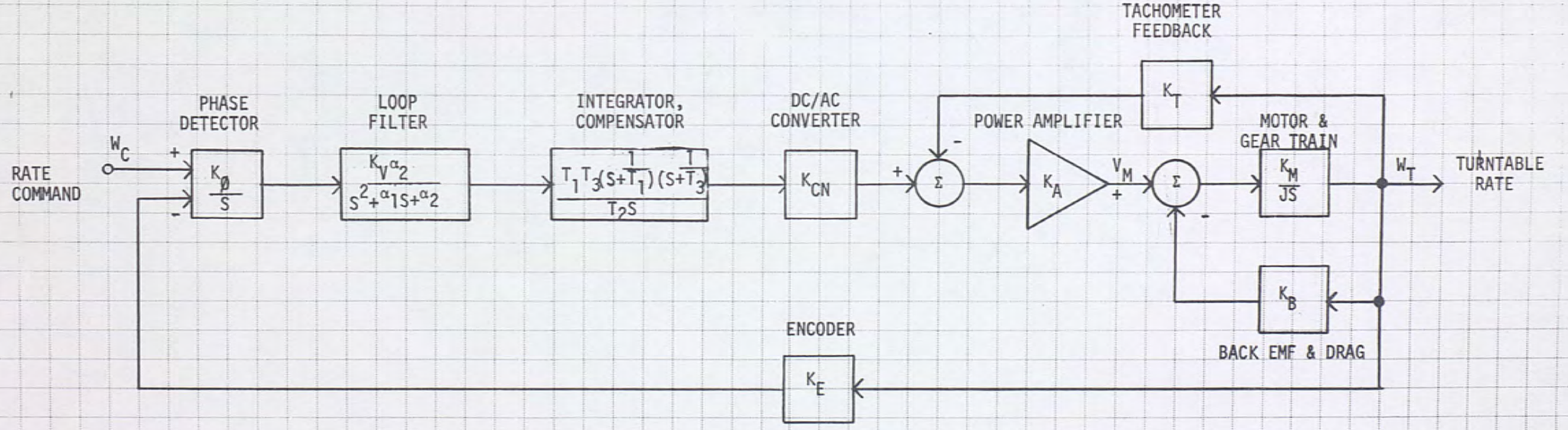

$$G(S) = \frac{K_\phi T_1 T_3 K_V \alpha_2 K_{CN} K_A K_M}{JT_2} \frac{(S+\frac{1}{T_1})(S+\frac{1}{T_3})}{S^2(S^2+\alpha_1 S+\alpha_2)} \frac{1}{S+K_M(K_B+K_A K_T)}$$

$$H(S) = K_E$$

Substitute: & $T_3 = \frac{J}{K_M(K_B+K_A K_T)}$

$$T(S) = \frac{W_T}{W_C} = \frac{G(S)}{1+G(S)\,H(S)}$$

$$T(S) = \frac{2.881 \cdot 10^2 (S+4.809 \cdot 10^1)}{S^4+3.284 \cdot 10^2 S^3+5.391 \cdot 10^4 S^2+5.185 \cdot 10^6 S+2.494 \cdot 10^8}$$

Poles follow fourth order Butterworth; F_B = 20Hz

FIGURE 3.6

LOOP CONSTANTS:

$K_\phi = 0.1194 \frac{VDC}{RAD}$

$T_1 = 2.079 \cdot 10^{-2}$ (SEC)

$T_2 = 2.150 \cdot 10^{-1}$ (SEC)

$T_3 = 2.264 \cdot 10^{-4}$ (SEC)

$K_V = 8.837 \frac{VDC}{VDC}$

$\alpha_1 = 3.284 \cdot 10^2 \frac{1}{SEC}$

$\alpha_2 = 5.391 \cdot 10^4 \frac{1}{SEC}$

$K_{CN} = 0.5 \frac{VAC}{VDC}$

$K_A = 136.36 \frac{VAC}{VAC}$

$K_T = 9.5113 \frac{VAC}{RAD/SEC}$

$K_M = 5.77 \frac{IN\text{-}LB}{VAC}$

$K_B = 53.11 \frac{VAC}{RAD/SEC}$

$J = 37.41$ IN-LB-SEC^2

$K_E = 18000. \frac{RAD}{RAD}$

The loop and its degree of stability may be better understood by considering figure 3.7, the root locus plot of the characteristic equation of the system. Equations (3.15), (3.29) and (3.30) yield:

$$G(S)H(S)= \frac{K_{CL}(S+4.809\cdot 10^{1})}{S^{2}(S^{2}+3.284\cdot 10^{2}S+5.391\cdot 10^{4})} \qquad (3.32)$$

By inspection of (3.32):

$$Z = 1;\ P = 4,$$

Therefore:

$$N = 4$$

Where, Z = number of finite zeros of $G(S)\ H(S)$;

P = number of finite poles of $G(S)\ H(S)$;

N = number of root loci

The four poles of $G(S)\ H(S)$ are shown in figure 3.7, and are at $S=0$, $S=0$, $S=164.18 + j\ 164.18$, and $S=164.18-j164.18$. The zero of $G(S)\ H(S)$ is at $S = 48.09$. The actual roots of the characteristic equation are shown at $S=116.10 \pm j\ 48.09$, and $S=48.09 \pm j\ 116.10$ (4th order Butterworth poles).

The three asymtotes for the root loci were constructed as follows:

$$\alpha_{1}= \frac{\Sigma\text{poles of } G(S)H(S) - \Sigma\text{zeros of } G(S)H(S)}{P - Z} \qquad (3.33)$$

$$\Theta_{R} = \frac{(2K+1)180^{\circ}}{P-Z}\ , \text{ where } K=0,\ 1,\ \ldots,\ P-Z-1 \qquad (3.34)$$

where σ_{1}= intersection of asymtotes; Θ_{R}= angle of asymtotes.

therefore:

$$\sigma_{1}=\frac{(-164.18+j164.18-164.18-j164.18) - (-48.09)}{3}$$

$$\sigma_{1}= -93.42 \qquad (3.35)$$

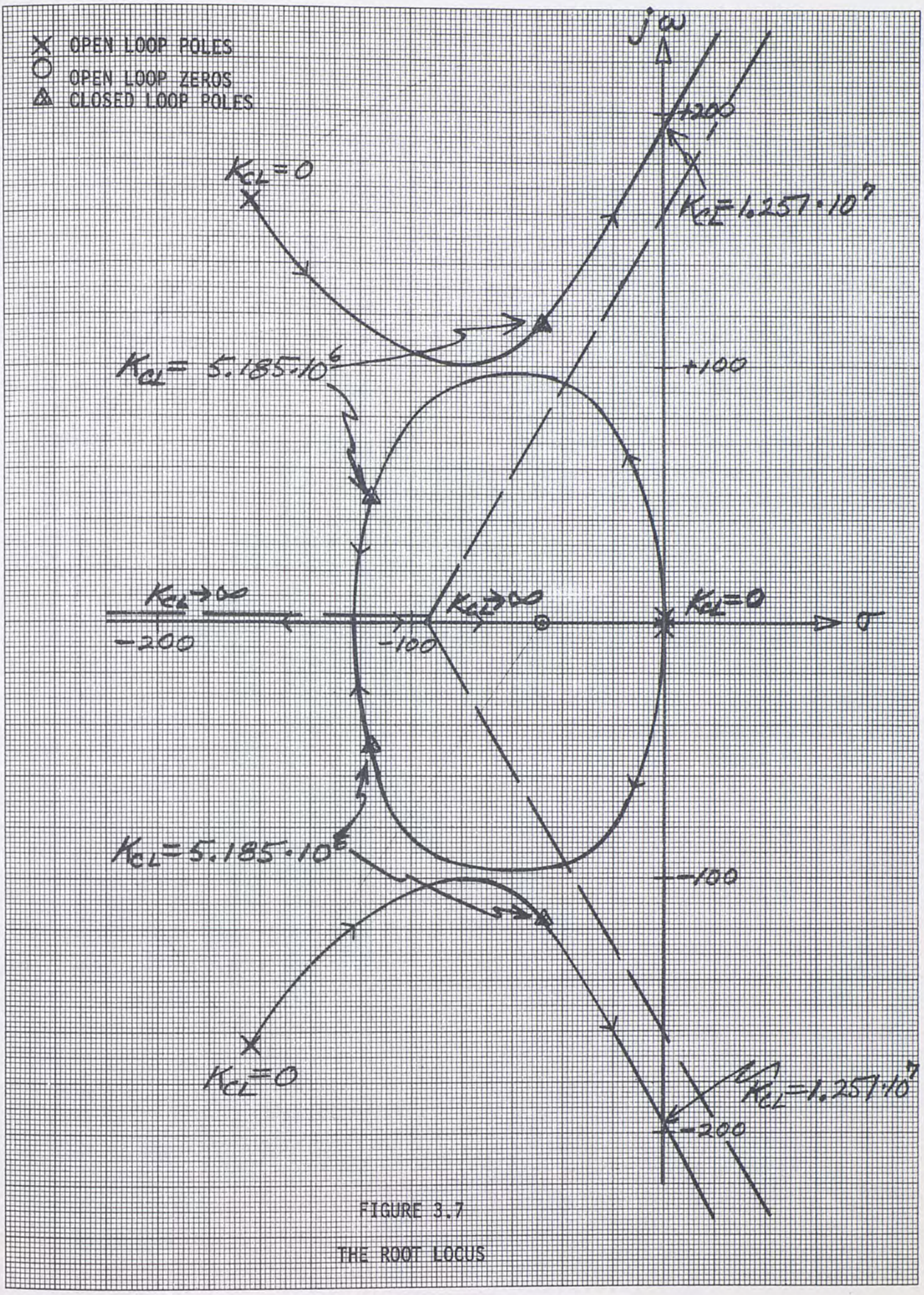

FIGURE 3.7

THE ROOT LOCUS

$$\Theta_1 = \frac{180°}{3} = 60° \tag{3.36}$$

$$\Theta_2 = \frac{3(180°)}{3} = 180° \tag{3.37}$$

$$\Theta_3 = \frac{5(180°)}{3} = 300° = -60° \tag{3.38}$$

Breakaway points from the real axis may be found by solving the following equation for S.

$$\frac{d}{ds} \left(G[S]\, H[S]\right) = 0 \tag{3.39}$$

Therefore:

$$\frac{d}{ds} \frac{K_{CL}\,(S+4.809\cdot 10^1)}{S^2(S^2+3.284\cdot 10^2 S+5.391\cdot 10^4)} = 0 \tag{3.40}$$

Applying the chain rule and the quotient rule for differention, (3.40) may be reduced to:

$$S(S^3+2.831\cdot 10^2 S^2+3.376\cdot 10^4 S+1.728\cdot 10^6) = 0 \tag{3.41}$$

Two real solutions to equation (3.41) can be easily shown to be S=0 and S= -122.68. These points are shown in figure 3.7.

Routh's Criterion may be used to determine the closed loop gain (K_{CL}) and the frequency at which the loci will intercept the imaginary axis. This point is of interest as it is the point of marginal loop stability.

The characteristic equation is:

$$S^4+3.284\cdot 10^2 S^3+5.391\cdot 10^4 S^2+K_{CL}S+4.809\cdot 10^1 K_{CL} = 0 \tag{3.42}$$

Then the Routh tabulation is:[2]

S^4	1	$5.391\cdot 10^4$	$4.809\cdot 10^1 K_{CL}$
S^3	$3.284\cdot 10^2$	K_{CL}	

$$S_2 \quad \frac{1.770 \cdot 10^7 - K_{CL}}{3.284 \cdot 10^2} \qquad 4.809 \cdot 10^1 K_{CL}$$

$$S^1 \quad K_{CL} \frac{(K_{CL} - 1.251 \cdot 10^7 K)}{1.770 \cdot 10^7 - K_{CL}} \qquad 0$$

$$S^0 \quad 4.809 \cdot 10^1 K_{CL}$$

Therefore, from the S^1 row:

$$K_{CL} = 1.251 \cdot 10^7 \tag{3.43}$$

From the S^2 row:

$$\frac{1.770 \cdot 10^7 - K_{CL}}{3.284 \cdot 10^2} + 4.809 \cdot 10^1 K_{CL} = 0 \tag{3.44}$$

Substituting (3.43) into (3.44) and rearranging, yields:

$$S^2 + 3.810 \cdot 10^4 = 0 \tag{3.45}$$

From which:

$$S = \pm j\ 195.20 \tag{3.46}$$

or,

$$W = 195.20 \text{ (RAD/SEC)} \tag{3.47}$$

These points of interception of the loci with the jw axis may be seen in figure 3.7.

Notice that the closed loop gain at phase-crossover is $K_{CL} = 1.251 \cdot 10^7$. The design gain ($K_{CL} = 5.185 \cdot 10^6$) may be divided into the phase-crossover gain to obtain the gain margin of the loop.

$$\text{Gain Margin (G.M.)} = 2.413 \tag{3.48}$$

or

$$\text{G.M.(dB)} = 7.650 \text{ dB} \tag{3.49}$$

[2] Benjamin C. Kuo, Automatic Control Systems (Englewood Cliffs, N.J.: Prentice-Hall, Inc., 1967), pp. 343-4.

This concludes the servo design of the velocity loop. It has been shown that the lags and constants can be chosen to arrive at a closed loop system with fourth order butterworth poles and over 100 percent gain margin. The next chapter will deal with the servo design of the position loop, and it will be shown that the loop can be designed to arrive at the same closed loop transfer function as the velocity loop.

CHAPTER IV

THE DESIGN OF THE POSITION SERVO LOOP

To begin the design of the position control loop, let us consider figures 2.1, 2.2, and 3.5. Figure 2.1 shows the block diagram of the position control system, and a comparison of figures 2.1 and 2.2 reveals that there is very little dynamic difference between the volocity and position loops. The major difference is in the feedback and error detection schemes.

Let us consider how figure 3.5 - the velocity servo loop dynamics - could be modified to model the performance of the position servo loop. The "intergrator/compensator", "loop filter", and "DC/AC converter" blocks could be identical, and the "turntable drive" block would require the addition of a "1/S" term to account for a positional output opposed to a velocity output. The feedback and error detector model would require modification as shown in Figure 4.1.

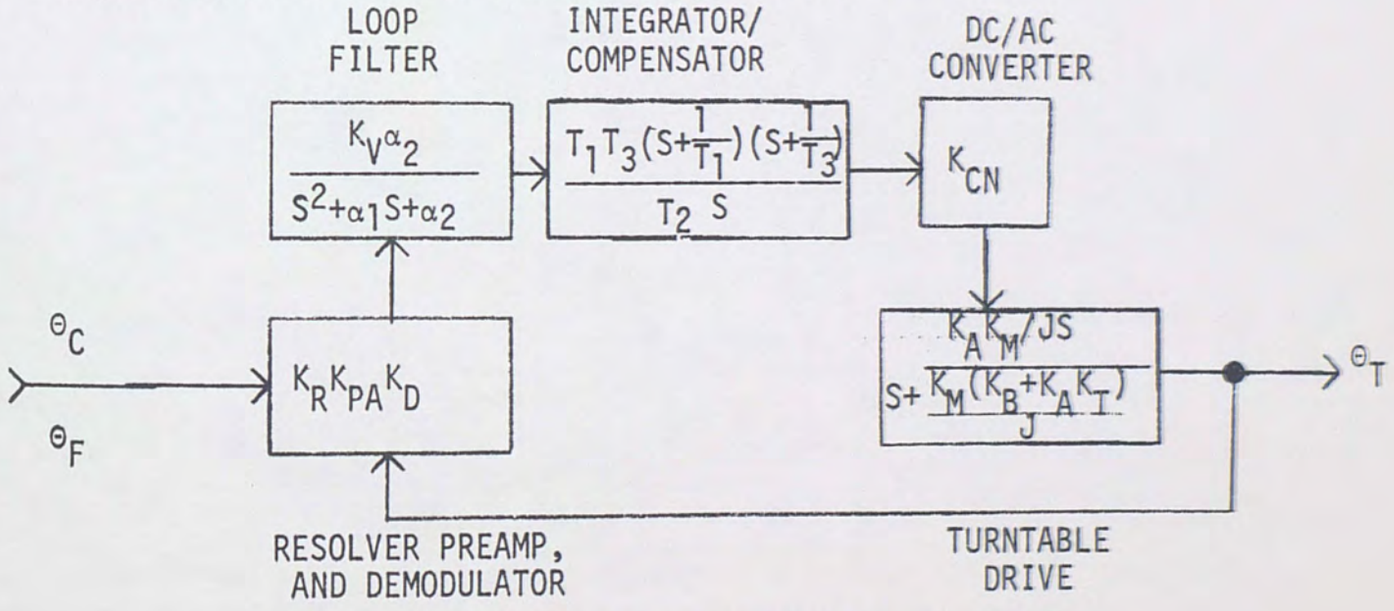

FIGURE 4.1 - THE POSITION SERVO LOOP DYNAMICS

Notice the extra "1/S" term in the drive block above. The resolver is modeled by showing unity position feedback, a summing junction, and the resolver gain in volts AC rms per radian. The two resolvers wired as shown in figure 2.1 actually subtract vectorially the feedback position from the command position to provide an error signal on one of the phases. This 400 cycle per second AC error voltage is amplified and then synchronously demodulated. The constant "K_R" accounts for resolver gain, "K_{PA}" is preamplifier gain, and "K_{CN}" is the demodulator gain.

In considering figures 4.1 and 3.5, it becomes evident that the forms - i.e. the format and order of terms - of the closed loop transfer functions for the two loops are identical. This fact can be used to great advantage if the closed loop transfer function of the position loop can be made numerically equivalent to that of the velocity loop.

The two main considerations in the design of the position loop dynamics are frequency response and noise suppression. Much consideration was given to the frequency response of the velocity loop as its mode of operation is dynamic. In contrast, once the position loop has rotated the turntable to the command position, the loop will be in a static condition. As for noise suppression, the loop will need to suppress 400 cycle per second ripple which will come from the coherent demodulator. The velocity loop was designed to adequately suppress 300 cycle per second noise. Using this reasoning, the transfer function of the velocity loop may be adopted for use as the position loop transfer function. This step will result in considerable commonality of circuitry between the two loops, saving much design and fabrication time, and resulting in an overall simplified system.

Referring to figure 4.1, the closed loop transfer function may be written as follows:

$$G(S)= \frac{(K_R K_{PA} K_0 T_1 T_3 K_V \alpha_2 K_{CN} K_A K_M)}{(T_2 J S^2)} \quad \frac{S+1/T_1}{S^2+\alpha_1 S+\alpha_2} \tag{4.1}$$

$$H(S) = 1 \tag{4.2}$$

$$K_{OL} = \frac{K_R K_{PA} K_D T_1 T_3 K_V \alpha_2 K_{CN} K_A K_M}{T_2 J} \tag{4.3}$$

$$K_{CL} = K_{OL} \tag{4.4}$$

$$T(S) = \frac{\Theta_T}{\Theta_C} = \frac{K_{OL}(S+1/T_1)}{S^4 + \alpha_1 S^3 + \alpha_2 S^2 + K_{CL} S + \frac{K_{CL}}{T_1}} \tag{4.5}$$

As before, the term '$(S+1/T_3)$' is assumed to have canceled with the term "$S+ \frac{K_M(K_B+K_A K_T)}{J}$", therefore equation (3.5) still holds.

$$T_3 = \frac{J}{K_M(K_B + K_A \cdot K_T)} \tag{3.5}$$

As before:

$$T_3 = 2.264 \cdot 10^{-4} (SEC) \tag{4.6}$$

Equations (3.13) through (3.16) still apply:

$$\alpha_1 = 3.284 \cdot 10^2 \tag{3.13}$$

$$\alpha_2 = 5.391 \cdot 10^4 \tag{3.14}$$

$$K_{CL} = 5.185 \cdot 10^6 \tag{3.15}$$

$$T_1 = 2.079 \cdot 10^{-2} \tag{3.16}$$

Equations (3.15) and (4.4) yield:

$$K_{OL} = 5.185 \cdot 10^{6} \tag{4.7}$$

To finalize the design, all knowns must be substituted into equation (4.3), and the remaining unknowns chosen. The following terms are knowns in equation (4.3), and are repeated here for convenience:

$$K_{OL} = 5.185 \cdot 10^{6} (RAD/RAD) \tag{4.7}$$

$$K_R = 26.0 \ (VAC/RAD) \tag{4.8}$$

$$T_1 = 2.079.10^{-2} (SEC) \tag{3.16}$$

$$T_3 = 2.264 \cdot 10^{-4} \ (SEC) \tag{4.6}$$

$$\sigma_2 = 5.391 \cdot 10^{4} \ (1/SEC^2) \tag{3.14}$$

$$K_{CN} = 0.50 \ (VAC/VDC) \tag{3.26}$$

$$K_A = 1500 \cdot (VAC/VAC) \tag{3.19}$$

$$K_M = 11.54 \ (IN\text{-}LB/VAC) \tag{3.21}$$

$$J = 37.41 \ (IN\text{-}LB\text{-}SEC^2) \tag{3.23}$$

$$K_{OL} = (K_R K_{PA} K_O T_1 T_3 K_V \alpha_2 K_{CN} K_A K_M) \tag{4.3}$$

$$5.185 \cdot 10^{6} = \frac{26 K_{PA} (KD)(2.08 \cdot 10^{-2})(2.26 \cdot 10^{-4})(K_V)(5.4 \cdot 10^{4})(.5)(1500)(11.5)}{T_2 (37.41)}$$

$$\frac{K_{PA} K_D K_V}{T_2} = 3.397 \cdot 10^{3} \tag{4.8}$$

The four constants in equation (4.8) may be chosen by considering the circuitry involved. The maximum resolver output is 26 volts AC, or 36.77 volts peak. Assuming the circuitry will saturate at about 12 volts, the preamplifier gain-to avoid saturation- should be:

$$K_{PA} = \frac{12}{36.77} = 3.264 \cdot 10^{-1} (VAC/VAC) \tag{4.9}$$

Again, to avoid saturation, the demodulator gain can be set at unity.

$$K_D = 1 (VDC/VAC) \tag{4.10}$$

For reasons which will become apparent in the circuity design chapter, let:

$$K_V = 23.85 \ (VDC/VDC) \tag{4.11}$$

Then, the remaining variable, T_2, is determined by substituting (4.9) through (4.11) into (4.8).

$$T_2 = 2.291 \cdot 10^{-3} \ (SEC) \tag{4.12}$$

A numerical solution for G(S), H(S), and T(S) is now readily obtained by substituting now known terms into (4.1), and (4.5). The result is:

$$G(S) = \frac{5.186 \cdot 10^6 (S + 4.809 \cdot 10^1)}{S^2 (S^2 + 3.284 \cdot 10^2 S + 5.391 \cdot 10^4)} \tag{4.13}$$

$$H(S) = 1 \tag{4.2}$$

$$T(S) = \frac{5.186 \cdot 10^6 (S + 4.809 \cdot 10^1)}{S^4 + 3.284 \cdot 10^2 S^3 + 5.391 \cdot 10^4 S^2 + 5.185 \cdot 10^6 S + 2.494 \cdot 10^8} \tag{4.14}$$

Note that the closed loop transfer function for the position loop (4.14) is identical to that of the velocity loop (3.31) with the exception of a command scale factor. This difference is due to the fact that the position loop employs unity feedback while the velocity loop does not. Figure 4.2 shows the position control loop, the closed loop transfer function, and tabulates the loop constants.

This will conclude the servo design chapter for the position loop. It has been shown that the same dynamics involved in the velocity loop can be applied directly to the position loop, saving design time and

providing commonality of electronics. This chapter has been much shorter than the preceding chapter, as it built upon much which was already done. The root locus and gain margin calculations apply directly to the position loop dynamics.

FIXTURE POSITION CONTROL LOOP

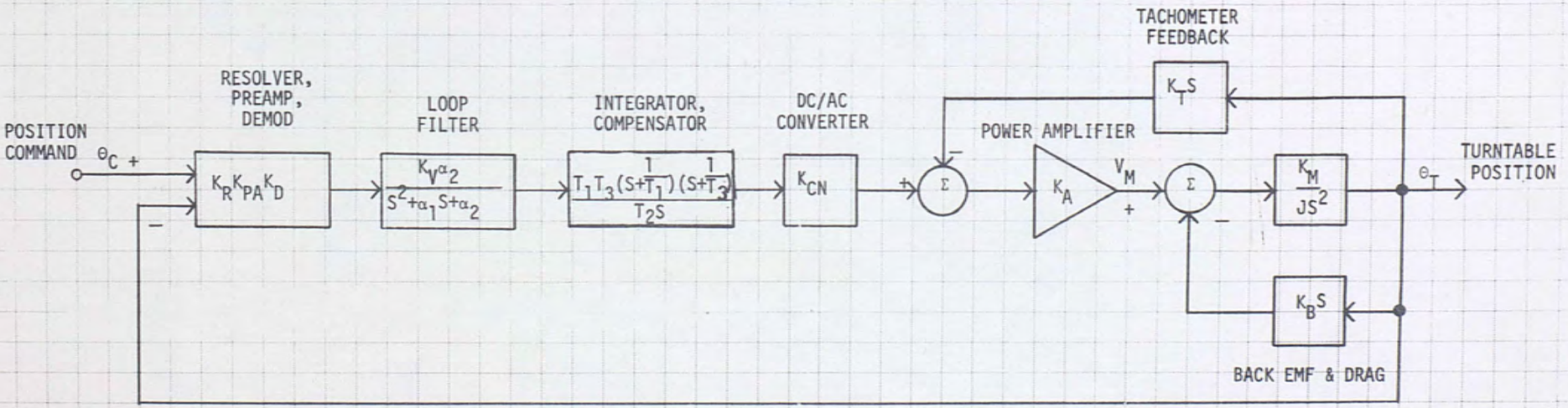

$$G(S) = \frac{K_R K_{PA} K_D T_1 T_3 K_V \alpha_2 K_{CN} K_A K_M}{JT_2} \cdot \frac{(S+\frac{1}{T_1})(S+\frac{1}{T_3})}{S^2(S^2+\alpha_1 S+\alpha_2)} \cdot \frac{1}{S+K_M(K_B+K_A K_T)}$$

$H(S) = 1$

Substitute: & $(T_3 = \frac{J}{K_M(K_B+K_A K_T)})$

$$T(S) = \frac{\theta_T}{\theta_C} = \frac{G(S)}{1+G(S)H(S)}$$

$$T(S) = \frac{5.186 \cdot 10^6 (S+4.809 \cdot 10^1)}{S^4+3.284 \cdot 10^2 S^3+5.391 \cdot 10^4 S^2+5.185 \cdot 10^6 S+2.494 \cdot 10^8}$$

Poles follow fourth order butterworth; F_B=20 Hz

LOOP CONSTANTS:

$K_R = 26 \frac{VAC}{RAD}$

$K_{PA} = 3.264 \cdot 10^{-1} \frac{VAC}{VAC}$

$K_D = 1 \frac{VDC}{VAC}$

$T_1 = 2.079 \cdot 10^{-2}$ SEC

$T_2 = 2.291 \cdot 10^{-3}$ SEC

$T_3 = 2.264 \cdot 10^{-4}$ SEC

$K_V = 23.85 \frac{VDC}{VDC}$

$\alpha_1 = 3.284 \cdot 10^2 \frac{1}{SEC}$

$\alpha_2 = 5.391 \cdot 10^4 \frac{1}{SEC^2}$

$K_{CN} = 0.5 \frac{VAC}{VDC}$

$K_A = 136.36 \frac{VAC}{VAC}$

$K_T = 9.5113 \frac{VAC}{RAD/SEC}$

$K_M = 5.77 \frac{IN\text{-}LB}{VAC}$

$K_B = 53.11 \frac{VAC}{RAD/SEC}$

$J = 37.41$ IN-LB-SEC^2

FIGURE 4.2

CHAPTER V

THE DESIGN OF THE SERVO ELECTRONICS

Now that the servo analysis has been completed, and the desired transfer functions for each loop have been defined, the electronic circuitry necessary to implement the servo loops may be designed. To get started, we will present a functional block diagram (see Figure 5.1) of the system as it was implemented, and then we will consider the design of each block type. Finally the completed schematics of the electronic cards will be shown.

Consider first blocks 1, 2 and 3 shown in Figure 5.1. The wiring of the resolvers is as shown in Figure 2.1, and in Figure 5.2 the preamplifier - block 3 - is also shown. The servo will drive the turn table to cause nulls to occur on R1 - R3 of the control resolver, and

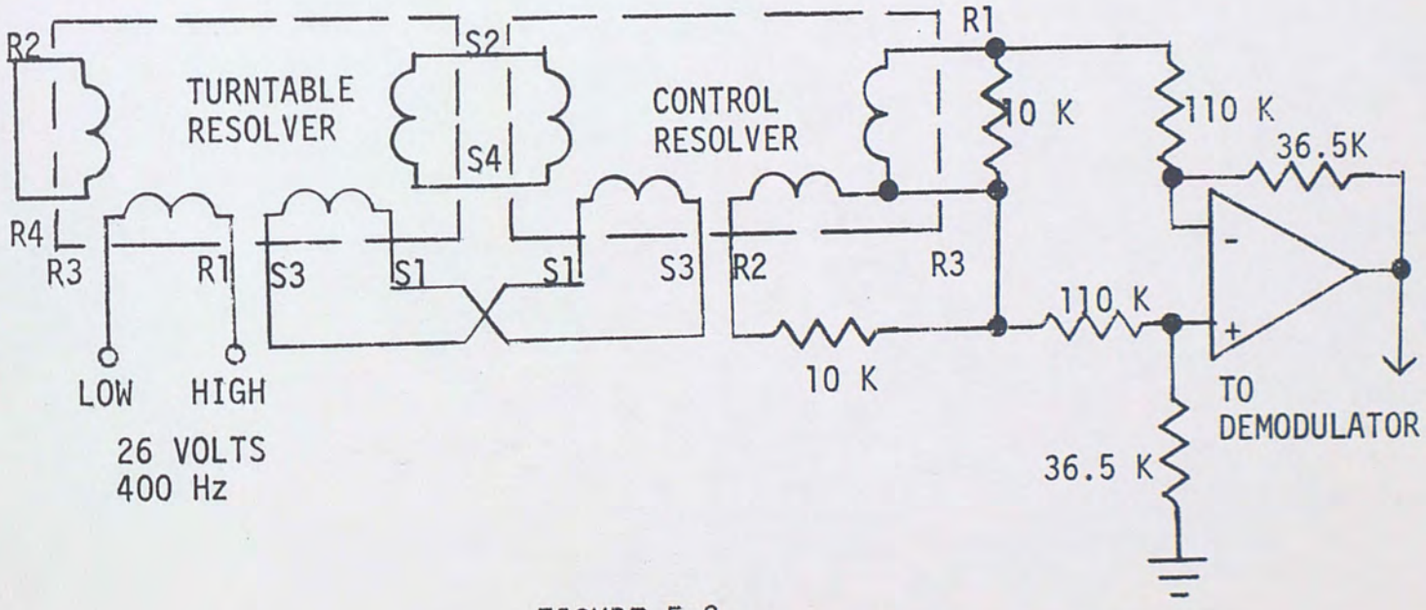

FIGURE 5.2

RESOLVER WIRING AND PREAMPLIFIER

FUNCTIONAL BLOCK DIAGRAM

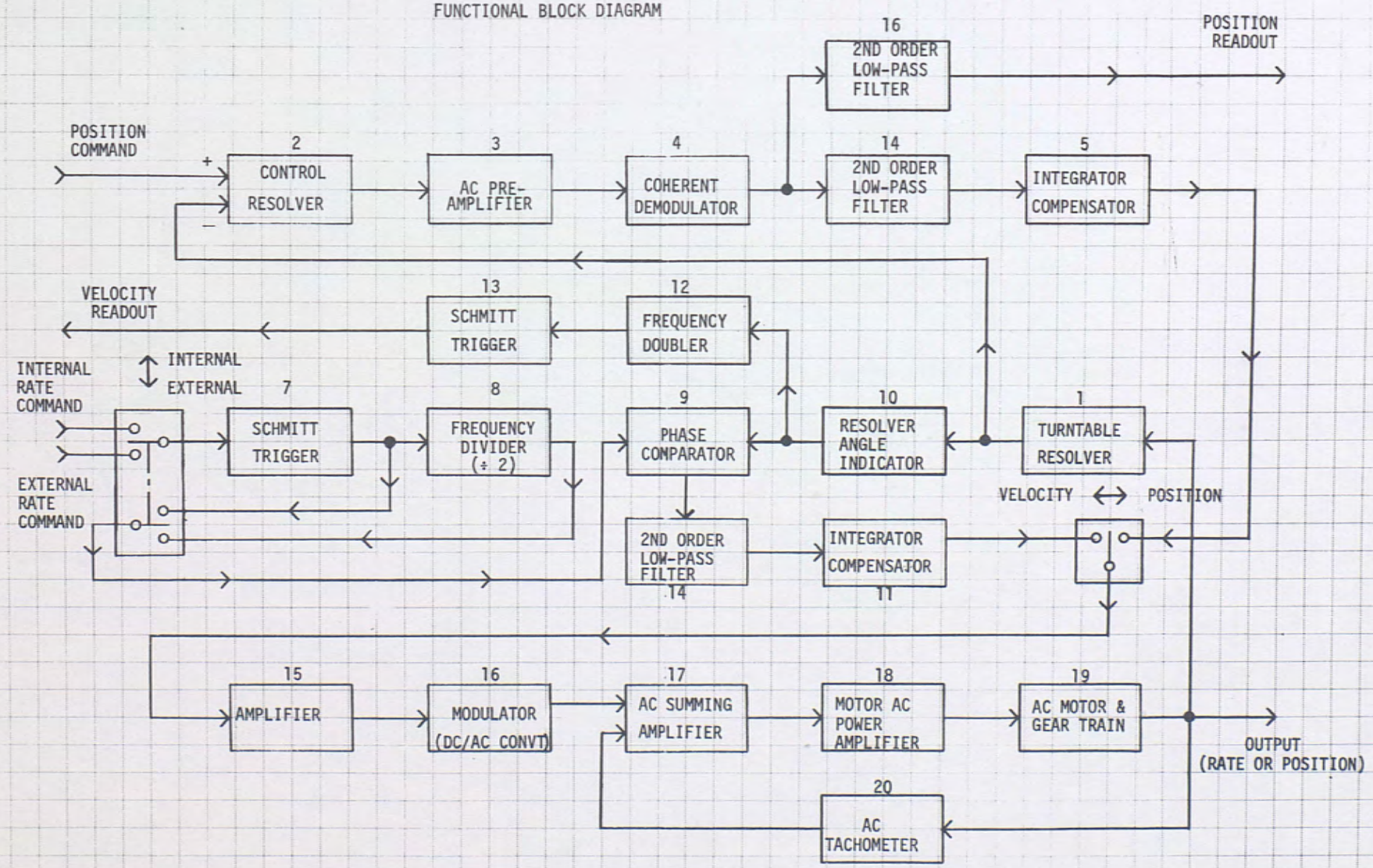

FIGURE 5.1

the position at which the null occurs may be adjusted by turning the control resolver. The two 10K ohm resisters shown are for equal loading of the phases. The amplifier shown is a differential amplifier employing a 741 operational amplifier. The gain of the amplifier is $3.318 \cdot 10^{-1}$ (VAC/VAC) - 36.5K/110K - and was chosen to prevent saturation at the peak resolver output.

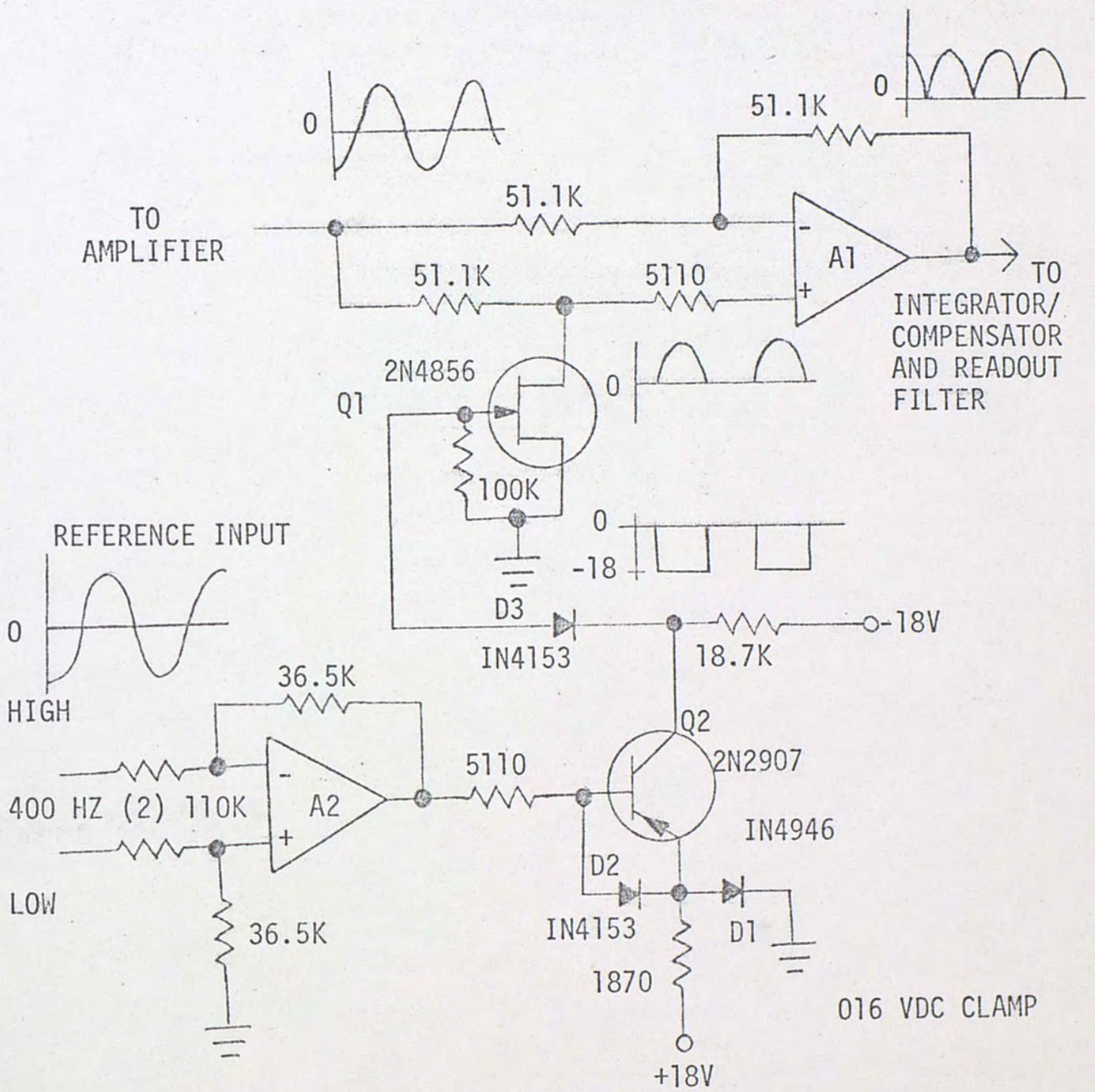

FIGURE 5.3

THE COHERENT DEMODULATOR

Figure 5.3 shows the implementation of block 4 - the coherent demodulator. Amplifier A1 is the heart of the demodulator. As Q1 - an FET Switch - switches on and off, the gain of A1 goes from (-1) to (+1). To better understand this, consider Figure 5.4. Figure 5.4(a) shows the conditions of A1 when Q1 is closed,

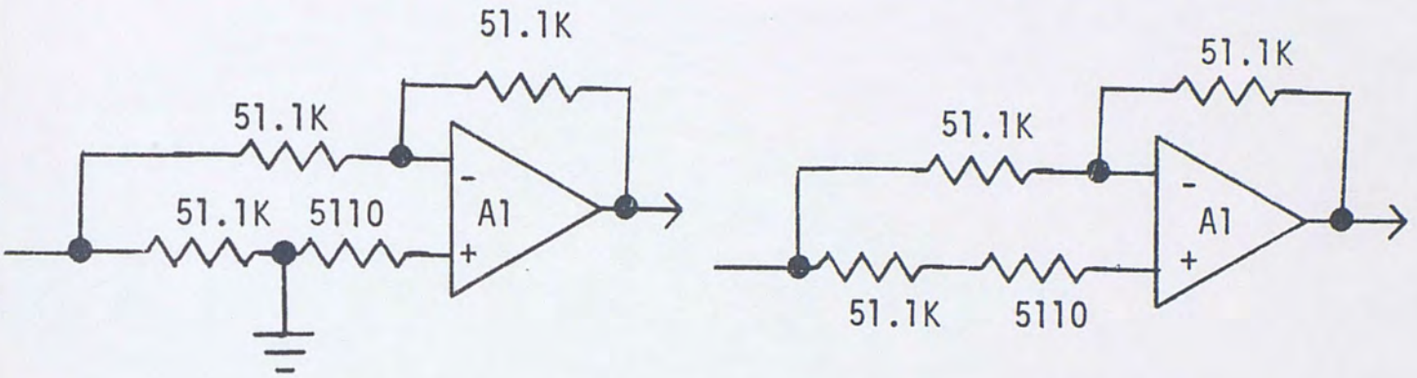

FIGURE 5.4

THE SWITCHING AMPLIFIER

and this is clearly an inverting op-amp with a gain of (-1). Figure 5.4(b) shows A1 when Q1 opens. Now we have a non-inverting configuration of gain (2) $-(1 + R_F/R_{IN})$ - superimposed with an inverting configuration of gain (-1) as above. The net result is a gain of (+1).

Getting back to Figure 5.3, amplifier A2 is identical to the pre-amplifier stage shown in Figure 5.1, and switches the collector of Q2. from about 0 to -18 volts. Diode D1 clamps the emitter of Q2 at 0.6 volts, and D2 protects the emitter-base junction of Q2 from back-bias voltages. D3 closes when Q2 goes off and Q1 goes off, thus switching

the amplifier gain as discussed above.

Consider now blocks 5 and 11 - the integrator/compensator. The circuit used for block 5 is shown in Figure 5.5(a). The gain of A1 may be determined as follows:

$$A_V = -Z_F/Z_{IN} \tag{5.1}$$

$$Z_F = \frac{R_1C_1S+1}{C_1S} \tag{5.2}$$

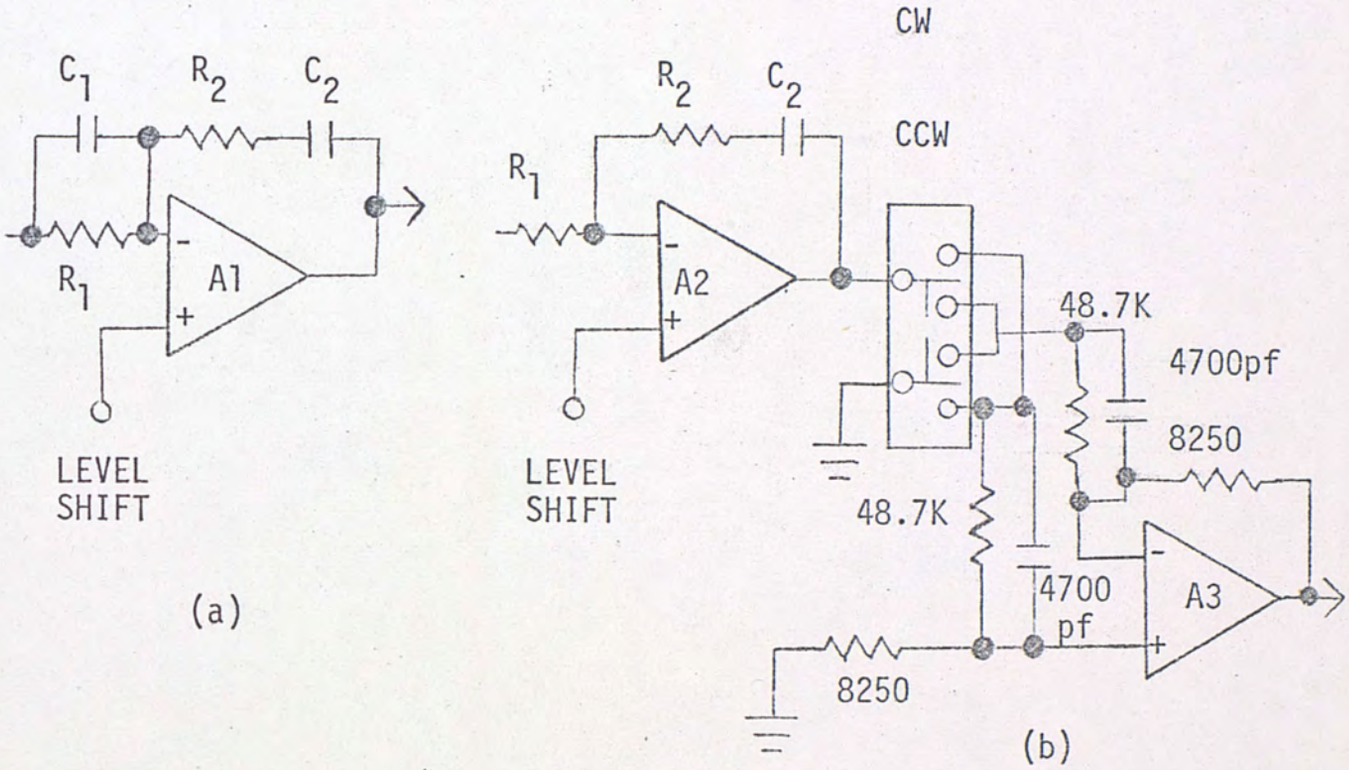

FIGURE 5.5
THE INTEGRATOR/COMPENSATOR

$$Z_{IN} = \frac{R_2}{R_2C_2S+1} \tag{5.3}$$

$$A_V = \frac{(1+R_1C_1S)(1+R_2C_2S)}{R_2C_1S} \tag{5.4}$$

The resistors and capacitors were chosen to implement the constants shown in Figure 4.2.

Figure 5.5(b) shows a slightly different circuit which was used in the velocity loop. The switch shown allows the loop gain to be reversed in sign in order to reverse the direction of rotation of the turntable.

Blocks 6 and 14 are as shown in Figure 5.6. The transfer function

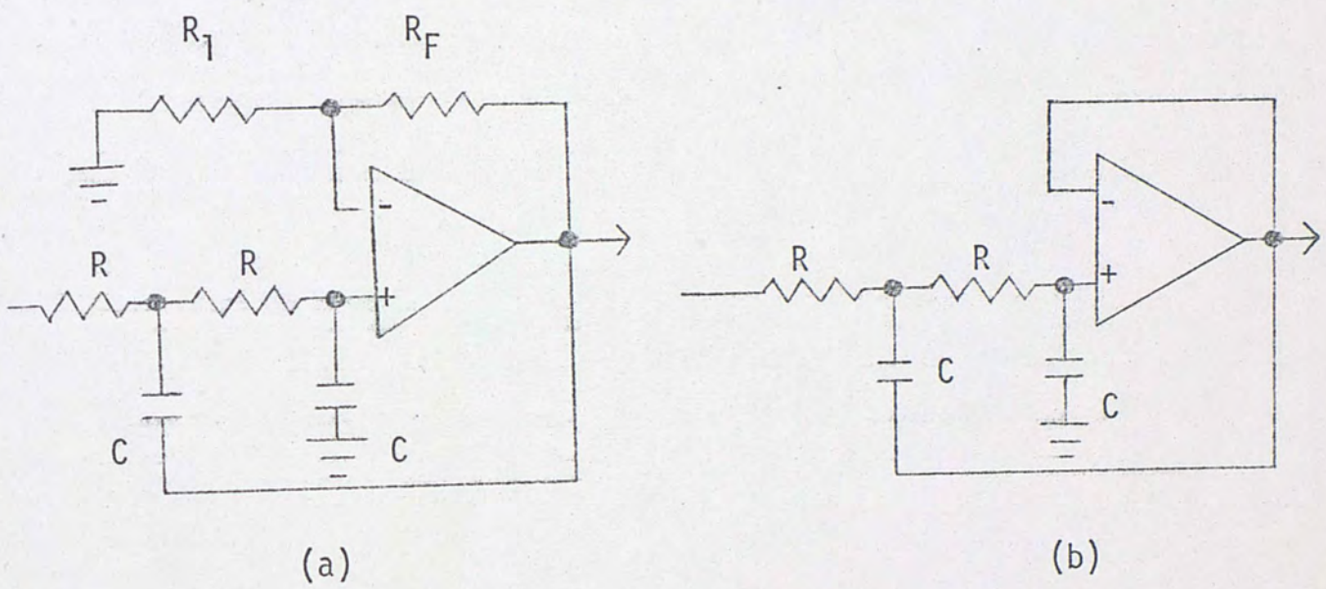

FIGURE 5.6

A SECOND ORDER BUTTERWORTH FILTER

of this type of circuit may be easily shown to be:

$$A_V(S) = \frac{K_V\ (1/RC)^2}{S^2 + \frac{(3-K_V)}{(RC)}\ S + (1/RC)^2} \qquad (5.5)$$

Where: $K_V = (1+R_F/R_1)$ (5.6)

In the case of Figure 5.6(b), K_y was set equal to unity, resulting in a simplification of the circuitry. Block 6 was built as in (b), and block 14 as in (a).

Figure 5.7 shows the command rate input circuitry - block 7 and 8. Amplifier A1 is the implementation of block 7. The output of A1 is a

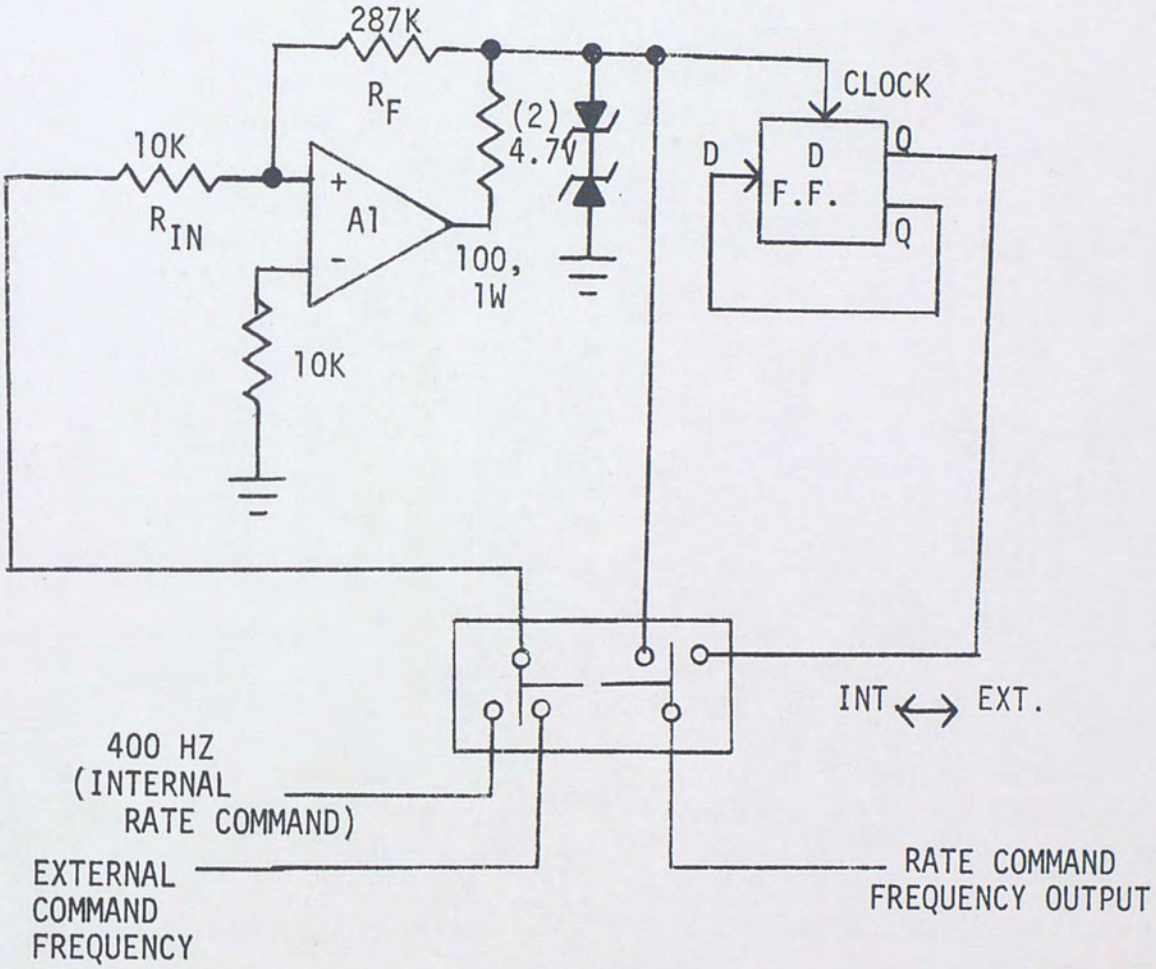

FIGURE 5.7

COMMAND RATE INPUT CIRCUITRY

square wave about 5 volts in amplitude (+ and -). The triggering level of the circuit is:

$$V_T \approx 5 \cdot \frac{R_{IN}}{R_F} = 0.17 \text{ VDC}$$

There are two modes of operation shown. The switch allows either the internal 400 HZ source to be used as a command source - in which case the turntable will rotate at 8 degrees per second - or an external frequency source may be selected - in which case the turntable will rotate at 0.01 degrees per cycle input. The purpose of the "D" flip flop is to divide the external input frequency by two to obtain a convenient input scale factor.

The output of figure 5.7 goes to a phase detector integrated circuit, where it is compared to the 0.01 degree output of the resolver angle indicator to generate an error voltage in volts per radian of phase error.

Blocks 12 and 13 come off of the 0.01 degree output of the resolver angle indicator, and their purpose is to generate pulses which may be counted by a counter in order to accurately measure the turntable rate of rotation. Figure 5.8 shows blocks 12 and 13. Although a detailed analysis of block 12 will not be presented, the wave forms at the input, output, and one intermediate point are shown. The input capacitor differentiates the square wave input to generate impulses which trigger the op-amp output to a "high" state. The amplifier remains in this state as long as V_3 remains above the +1.0 volt bias level. This time period is determined by the time constant: $\tau = R_1 C_1$, and the equation:

$$4.7\epsilon^{-t/\tau} = 1.0 \qquad (5.7)$$

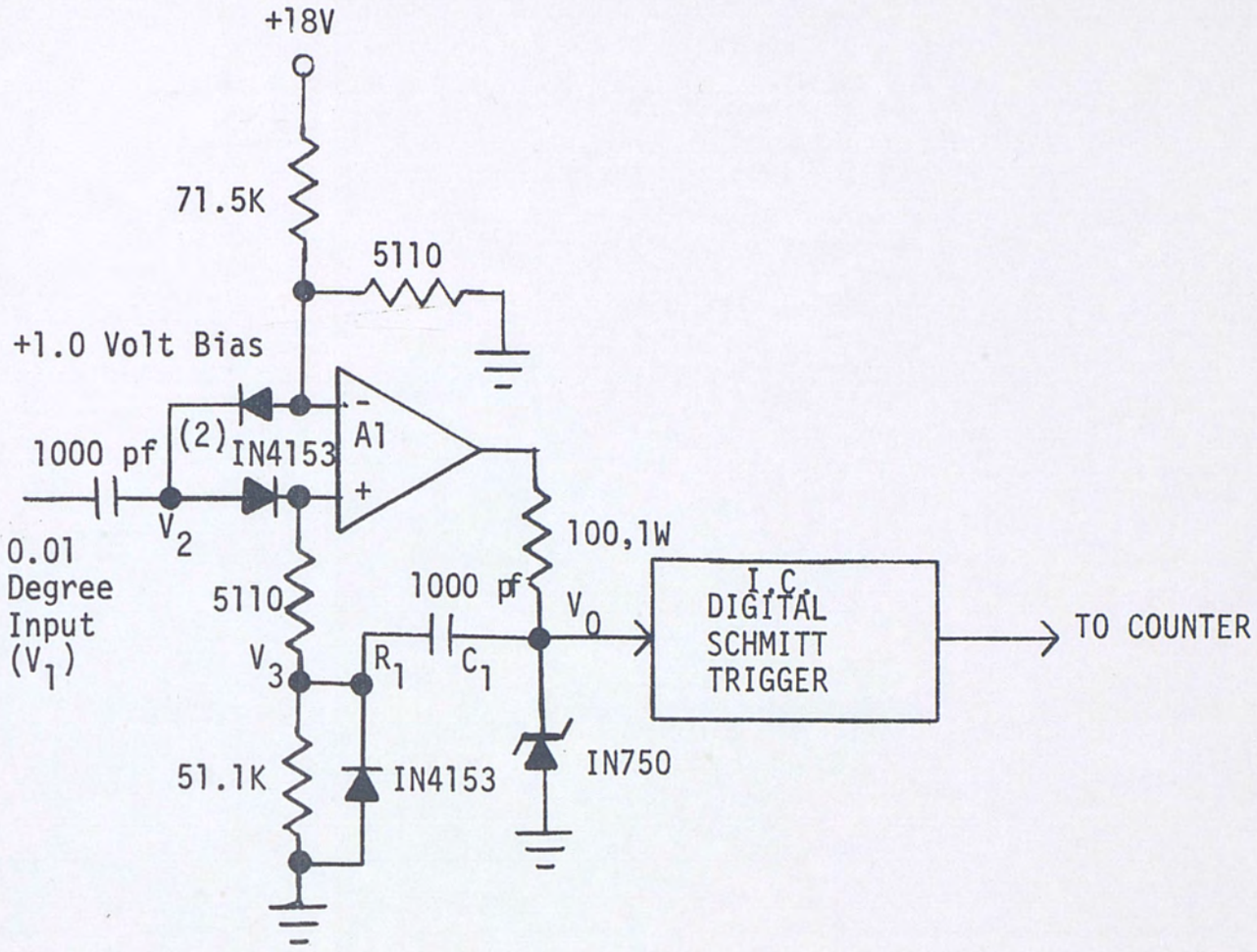

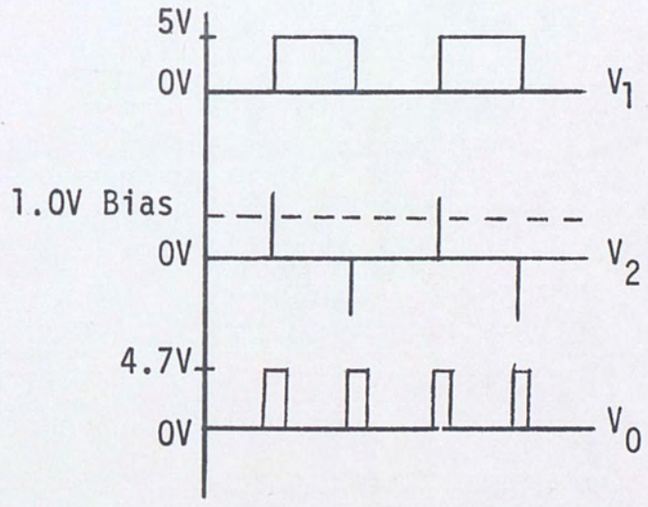

FIGURE 5.8

VELOCITY READOUT CIRCUITRY

The output of A1 is fed into a "fast" digital schmitt trigger, so that the pulses will be adequately "sharp" for a counter to detect. The resultant velocity readout output has a scale factor of 100 pulses per degree - or 100 Hz per degree per second.

Last among the electronics, let us consider blocks 15, 16, and 17. As shown in Figure 5.1, these blocks are common to both the velocity and position loops. Amplifier A1 in Figure 5.9 is a simple non-inverting operational amplifier with a gain of 15. The multiplier shown is used as a 400 cycle per second modulator. One input to the multiplier is a constant 5.0 VAC, 400 Hz. The other is a DC error signal (V_{DC}). The

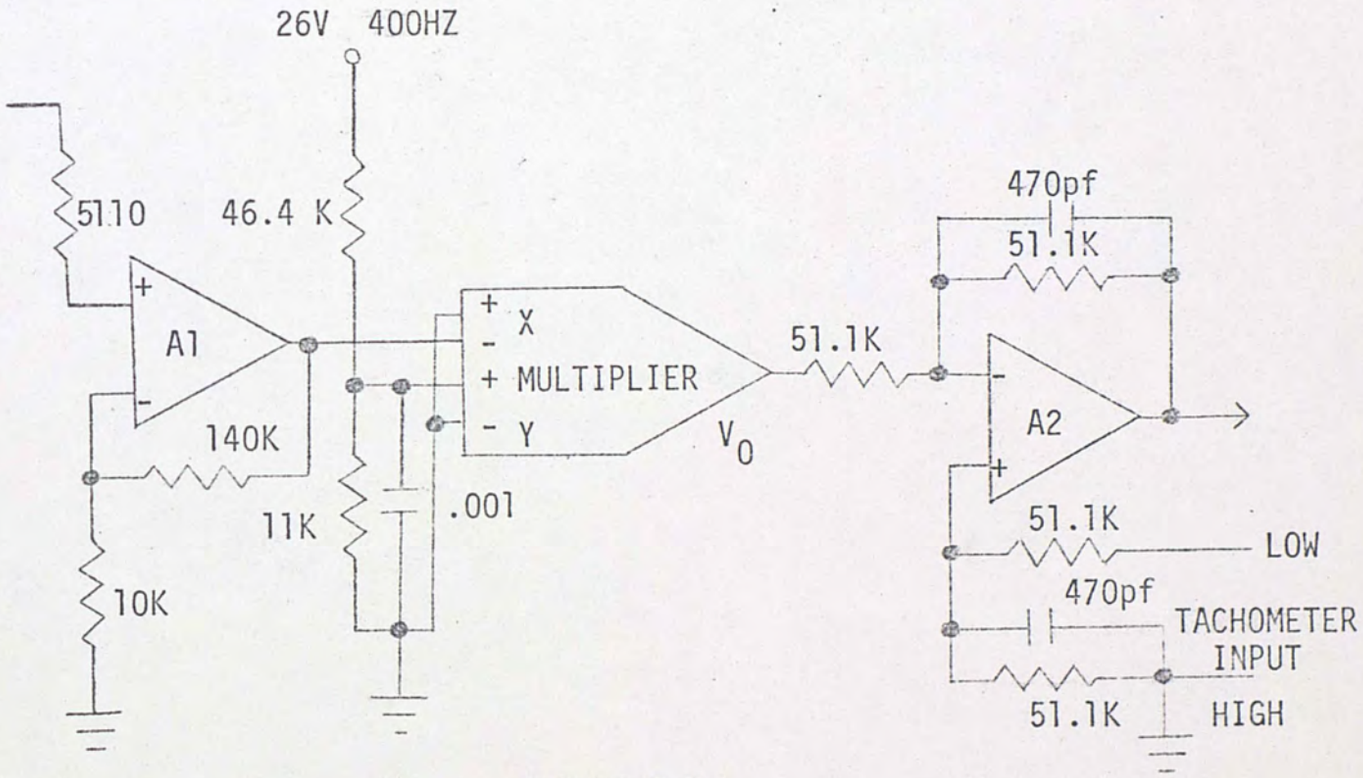

FIGURE 5.9

AMPLIFIER, MODULATOR, AND SUMMING

gain of the multiplier is:

$$V_O = \frac{V_X V_Y}{10} \tag{5.8}$$

Therefore:

$$V_O = V_{DC} 0.5 \text{ (VAC)} \tag{5.9}$$

and the modulator gain is:

$$A_V = 0.5 \text{ (VAC/VDC)} \tag{5.10}$$

Amplifier A2 is a differential amplifier of the type previously discussed. Its purpose is to provide a summing junction for the tachometer feedback (block 17). The 470 pf capacitors are for high frequency noise suppression.

Blocks 18, 19, and 20 represent a drive system which was purchased to drive the turntable, and therefore is not part of the electronics which was designed. Block 18 takes the output of figure 5.8 (or block 17) and amplifies it 1500 times. The output ranges from 0 to 36 volts AC, 400 Hz. and puts out up to 30 watts. The motor is a two phase 400 Hz induction motor. The pattern field is fixed at 115 VAC, 400 Hz., and the control field is center taped and driven by the power amplifier.

In this chapter, the types of circuitry used to implement the servo design were presented and explained in an attempt to complete the total system design picture. In order to show more clearly how the various circuits are interconnected, the actual schematics from which the two electronic control cards were built are shown in Figure 5.9 and 5.10. These circuits have been built and operate as intended. Appendix 1 contains some photographs of oscilloscope traces of the operation of the servo and associated circuitry.

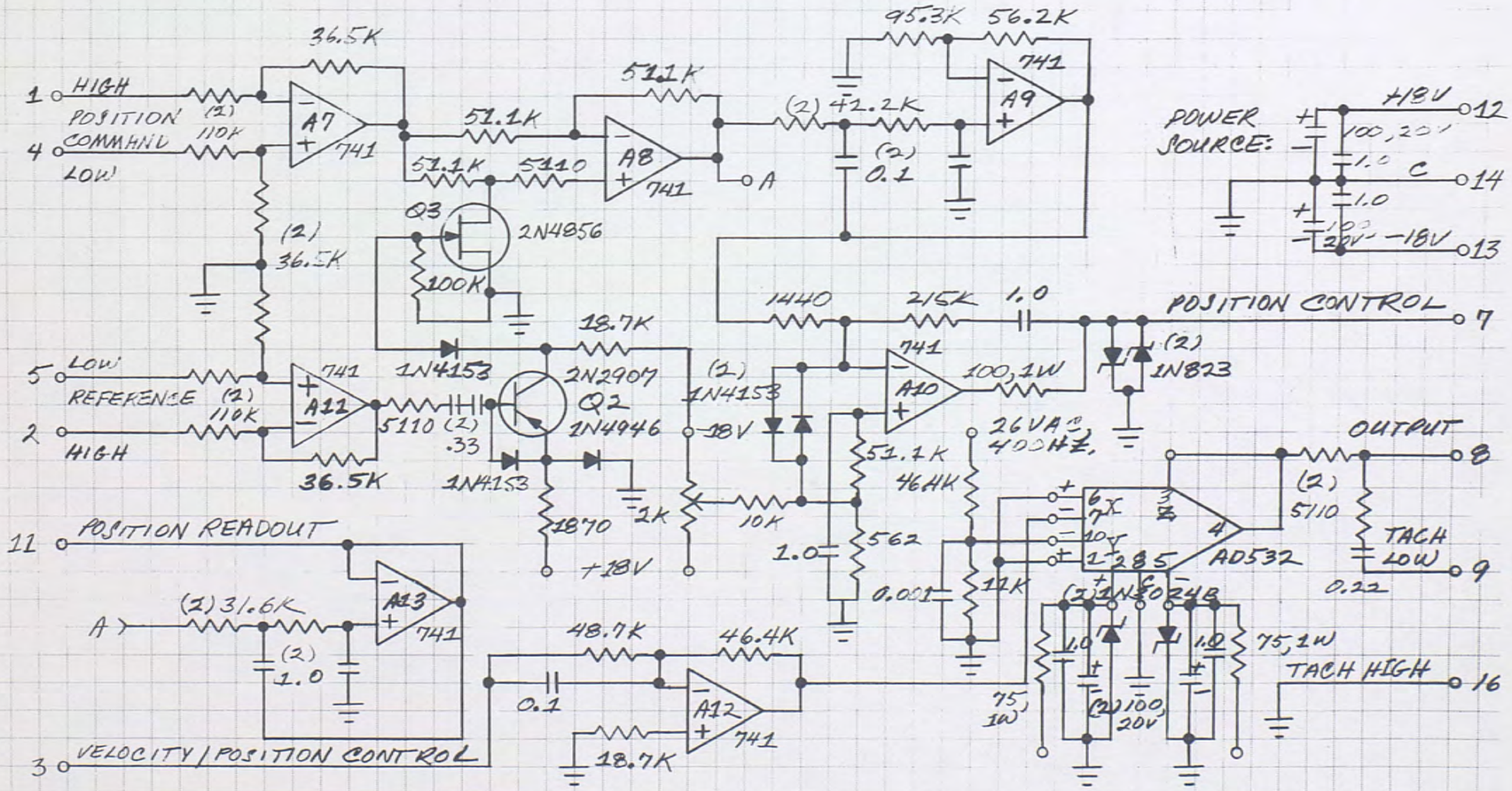
1
HIGH
POSITION
COMMAND
4
LOW
(2) 110K
36.5K
A7
741
51.1K
51.1K
5110
A8
741
A
95.3K
56.2K
741
A9
(2) 42.2K
(2) 0.1
POWER SOURCE:
+18V
12
100, 20V
1.0
C
14
1.0
100
20V
-18V
13
Q3
2N4856
100K
(2) 36.5K
1440
215K
1.0
POSITION CONTROL
7
18.7K
1N4153
2N2907
Q2
1N4946
5
LOW
REFERENCE
2
HIGH
(2) 110K
741
A11
5110
(2) .33
36.5K
1N4153
(2) 1N4153
-18V
741
A10
100, 1W
(2) 1N823
26VAC 400HZ
51.1K
46.4K
562
1.0
0.001
10K
1K
1870
+18V
11
POSITION READOUT
A
(2) 31.6K
(2) 1.0
A13
741
3
VELOCITY / POSITION CONTROL
48.7K
46.4K
0.1
A12
741
18.7K
AD532
OUTPUT
8
(2) 5110
TACH LOW
9
0.22
11K
(2) 1N4148
1.0
(2) 100, 20V
75, 1W
TACH HIGH
16
75, 1W

FIGURE 5.10

THE VELOCITY CONTROL ELECTRONICS

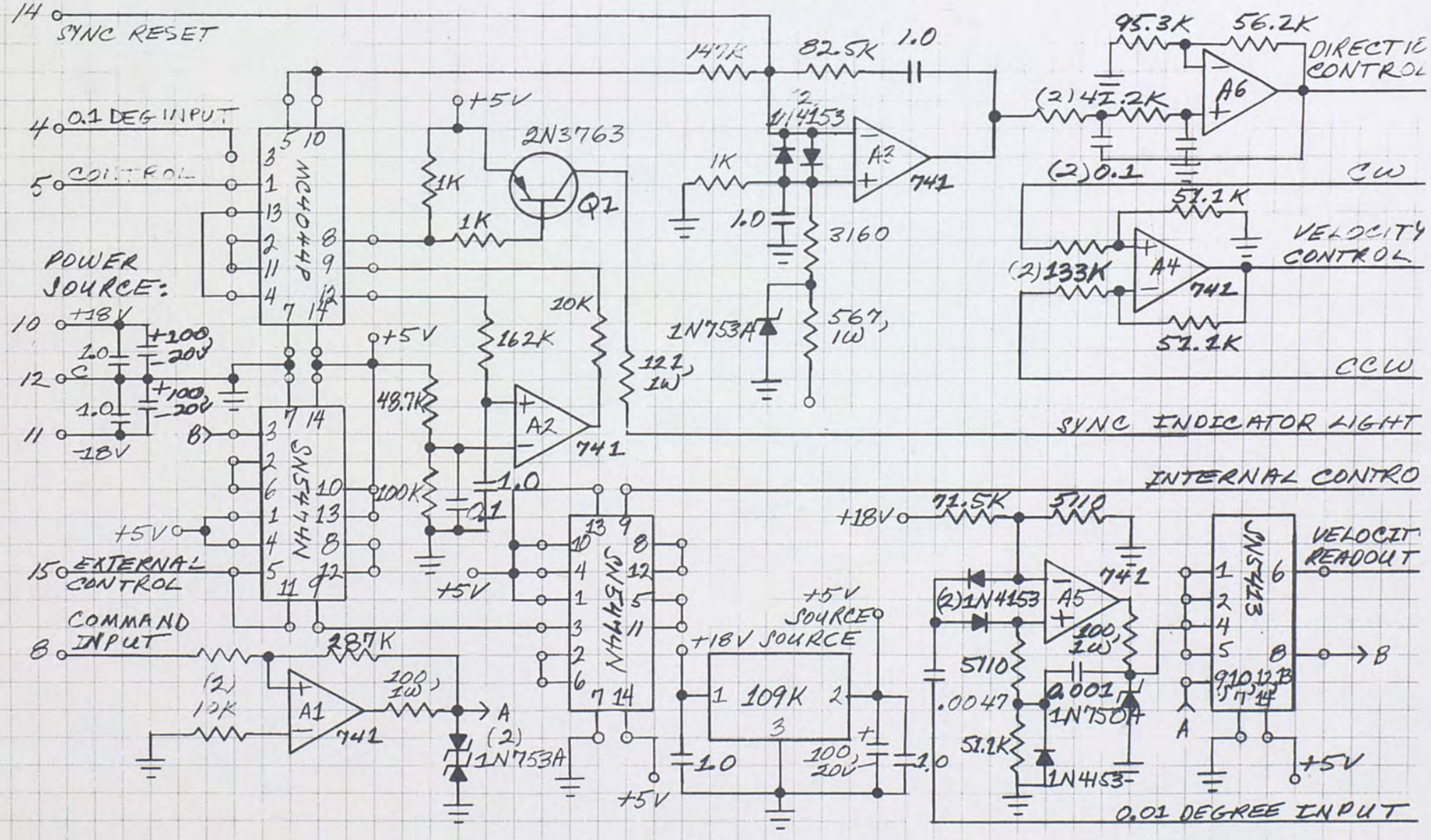

FIGURE 5.11

CHAPTER VI

SUMMARY AND CONCLUSIONS

The topic of this paper has been the design and fabrication of a servo controlled inertial sensor test fixture which was built by Martin Marietta Aerospace at Orlando. The primary purpose of this system was to add a remote control positioning capability to the high-g centrifuge test setup. The fixture and control panel allows the sensor under test to be positioned in any angle of the horizontal plane with respect to the acceleration vector, or to be maintained in a constant angular velocity mode, without requiring the centrifuge to be stopped and opened to do so.

A drawing of the velocity servo loop is shown in Figure 3.6. This loop was implemented as a phase locked loop which proved to be an excellent one, providing relative ease of design, and extreme accuracy. The command rate is entered as a frequency by a function generator or frequency synthesizer, and the turntable rate will track the input with zero steady state error due to the phase locked feature. The system was designed to operate from 6 to 12 degrees per second, but the actual hardware remains phase locked at rates from 1 to 16 degrees per second. The response of the system is adequate to maintain the phase locked condition while holding an inertial sensor at the highest acceleration levels of the centrifuge.

The fixture position control loop is shown in Figure 4.2. This loop was designed for commonality of circuitry with the velocity control loop, and it shares the same closed loop denominator polynomial and associated

frequency response.

The position command is entered by means of a control resolver, which sums with the feedback resolver to produce an input to the electronics. The angular position of the test sensor is read by a digital angle indicating device which operates off of the feedback resolver. In conjunction with a fine adjusting venier attached to the control resolver, angular adjustments may be made with a resolution of 0.01 degrees, and an accuracy of 0.05 degrees. There is an integrator in the open loop transfer function which eliminates any hangoff angle between the command and the feedback angles. Under high-g loading the fixture turntable tracks the position command to the nearest 0.01 degree as displayed by the angle indicator. The position overshoot is acceptable, with a settling time on the order of one half second.

The implementation of the servo design was made easy through the use of some modern integrated circuits such as 741 operational amplifiers and the phase detector. The schematics of the two electronic cards which were built are shown in Figures 5.10 and 5.11.

The intent of this paper has been to summarize the entire design picture for this project, from the conception of the system through its realization. Chapter I explains the need for the design and the design goals in a broad sense. Then, Chapter II goes into a consideration of design alternatives, and defines the format of the system. Chapters III and IV deal with the servo analysis conducted for the two control loops, and Chapter V completes the picture by describing how the control equations may be implemented electronically. Finally, photographs of the hardware are shown in the appendix.

APPENDIX

Photos and Oscilloscope Traces of the System and Its Operation

THE FIXTURE SERVO CONTROL PANEL - FRONT VIEW

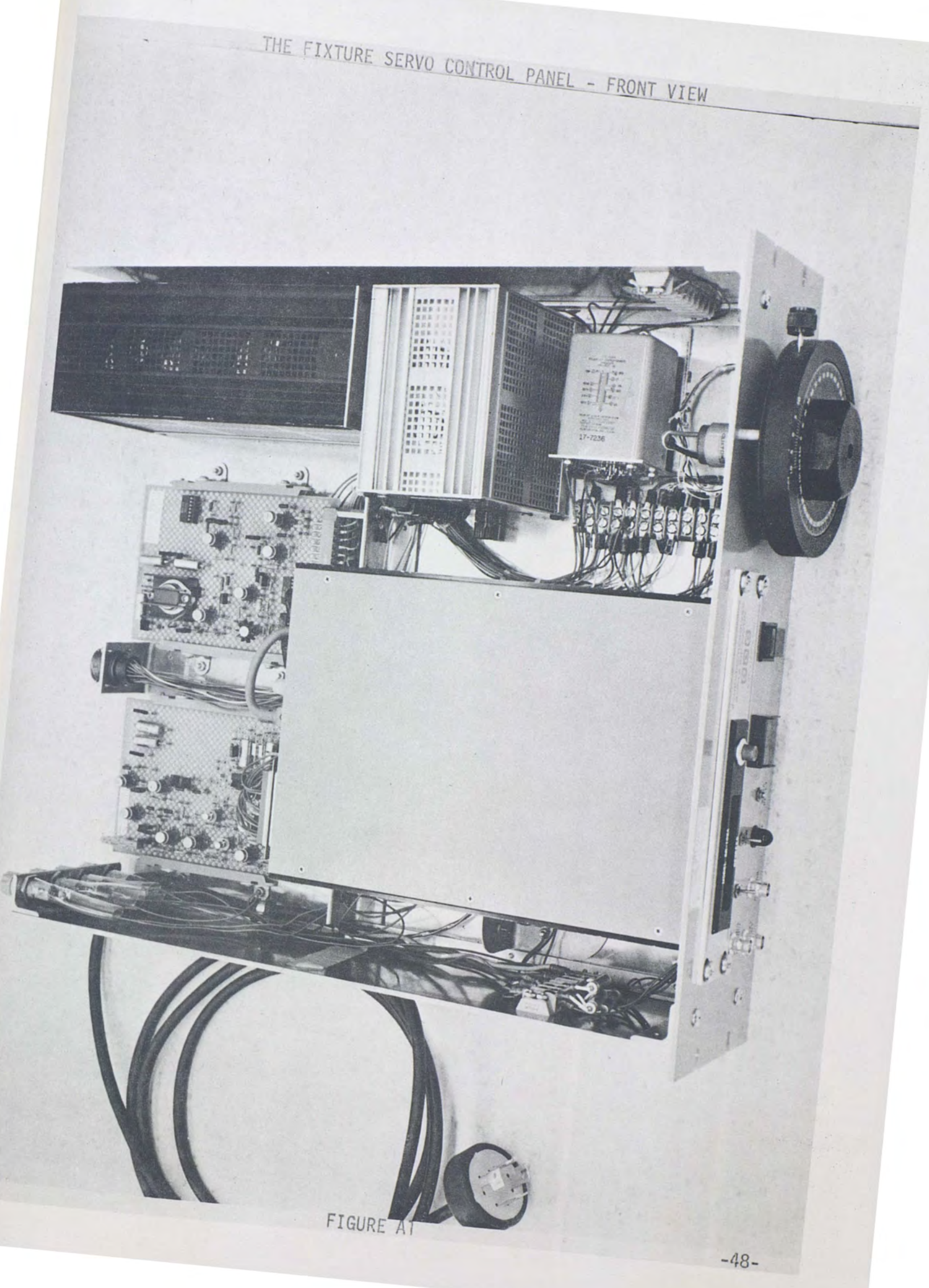

FIGURE A1

THE FIXTURE SERVO CONTROL PANEL - REAR VIEW

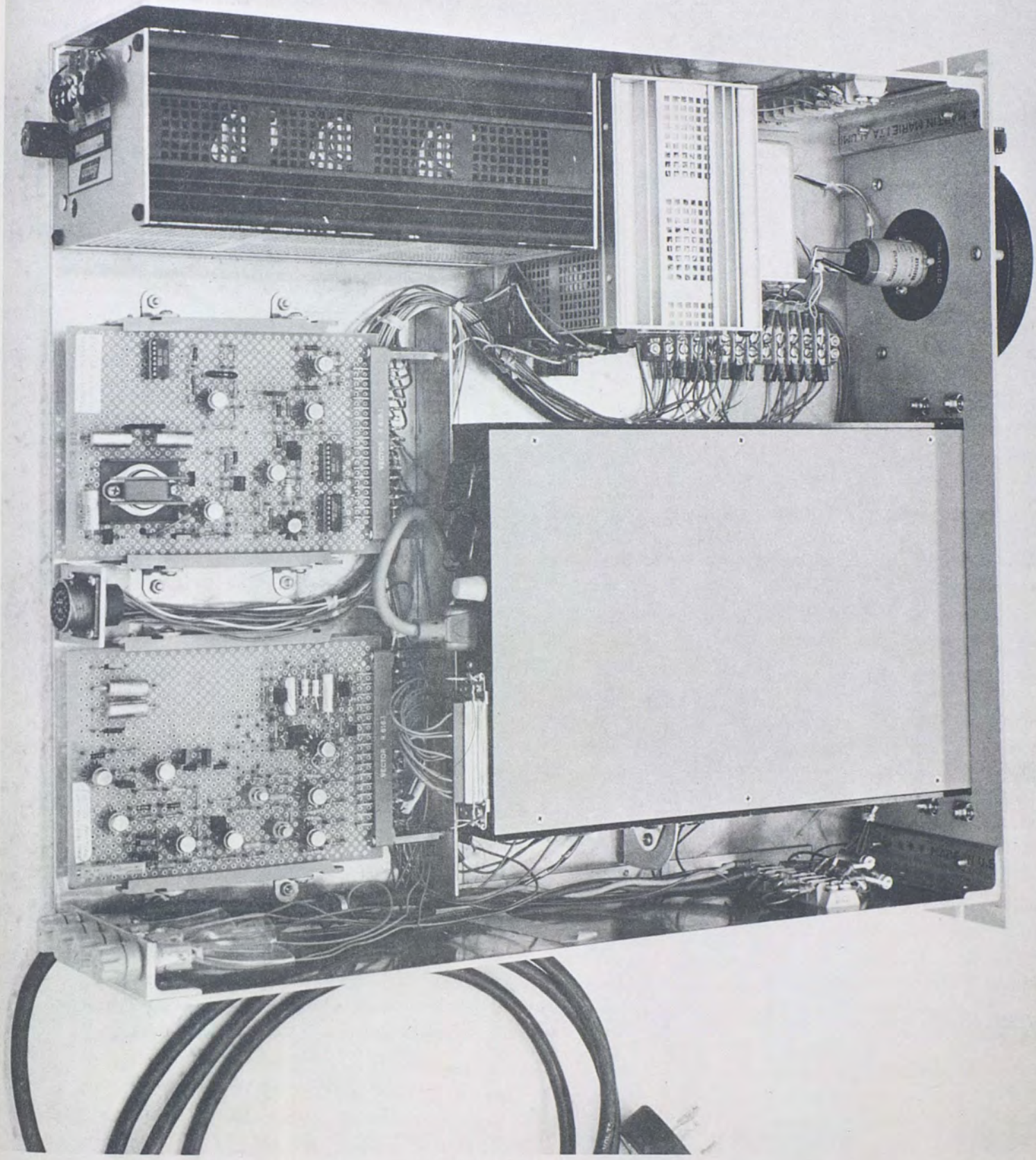

FIGURE A2

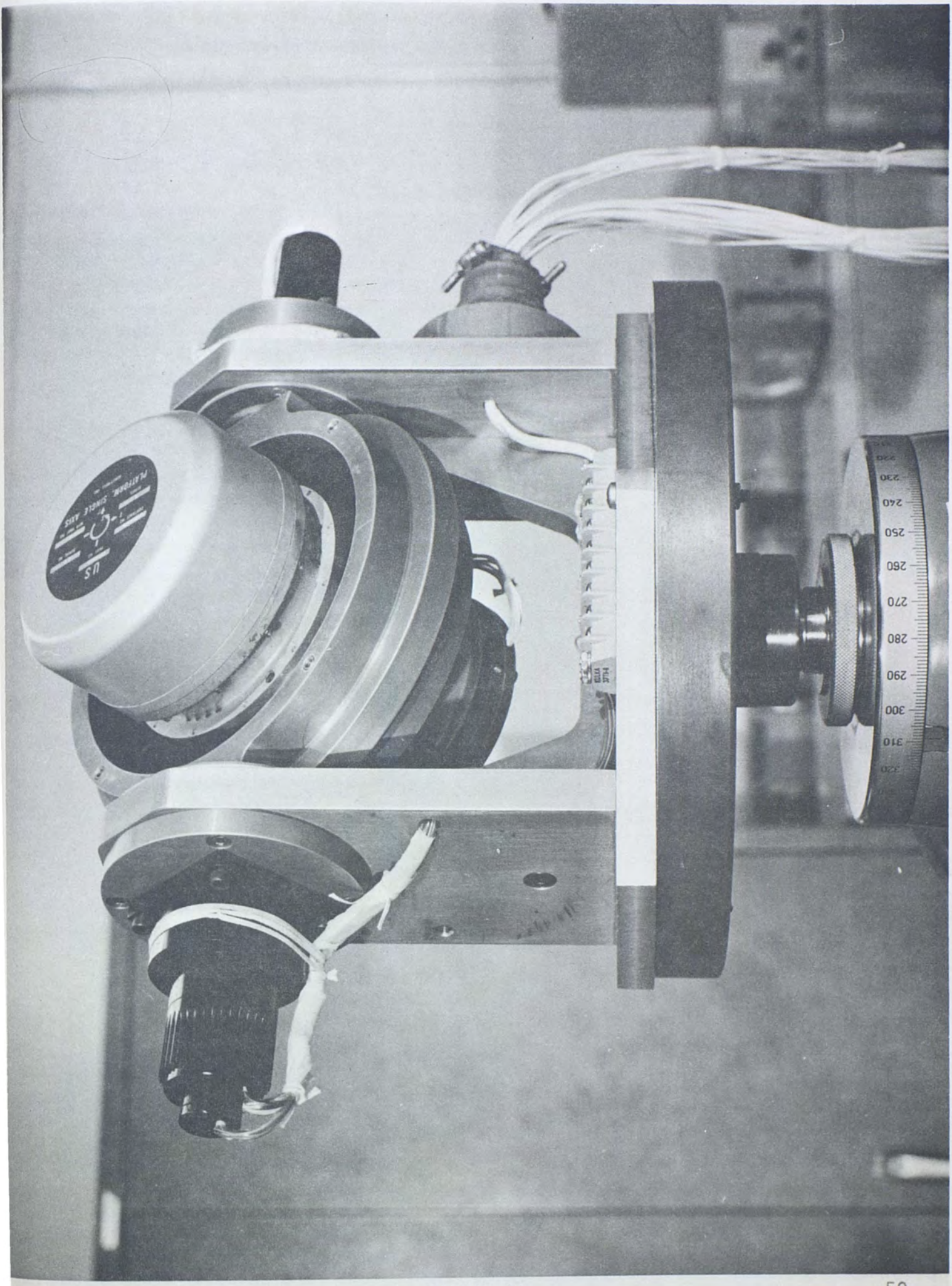

FIGURE A3

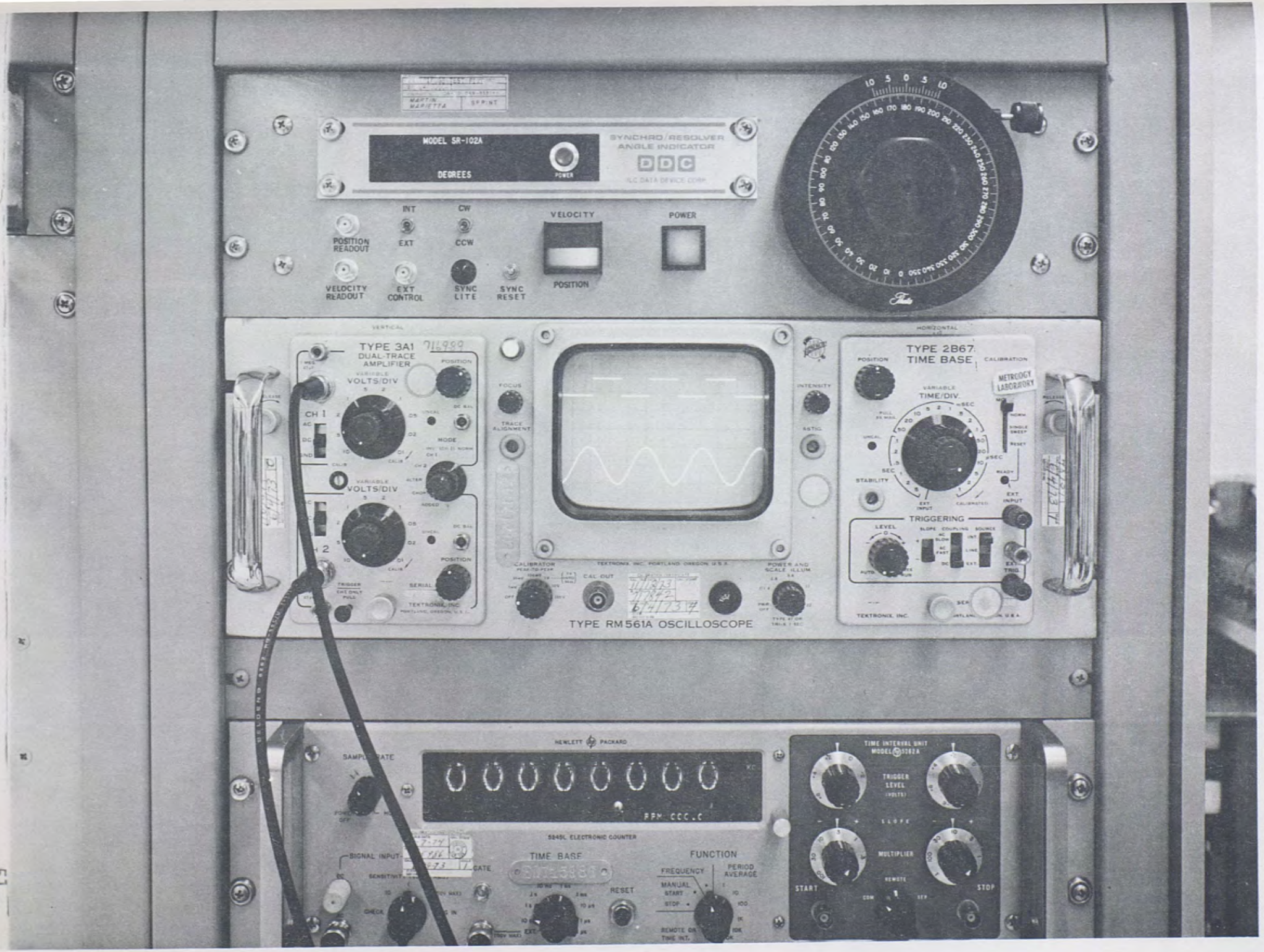
MODEL SR-102A
DEGREES
POWER
SYNCHRO/RESOLVER
ANGLE INDICATOR
DDC
INT
EXT
CW
CCW
POSITION READOUT
VELOCITY READOUT
EXT CONTROL
SYNC LITE
SYNC RESET
VELOCITY
POSITION
POWER
TYPE 3A1
DUAL-TRACE
AMPLIFIER
VOLTS/DIV
CH 1
CH 2
TYPE 2B67
TIME BASE
TIME/DIV.
TRIGGERING
TYPE RM561A OSCILLOSCOPE
HEWLETT PACKARD
5245L ELECTRONIC COUNTER
TIME BASE
FUNCTION
FREQUENCY
PERIOD AVERAGE
RESET
TIME INTERVAL UNIT
MODEL 5262A
TRIGGER LEVEL
SLOPE
MULTIPLIER
START
STOP

FIGURE A4

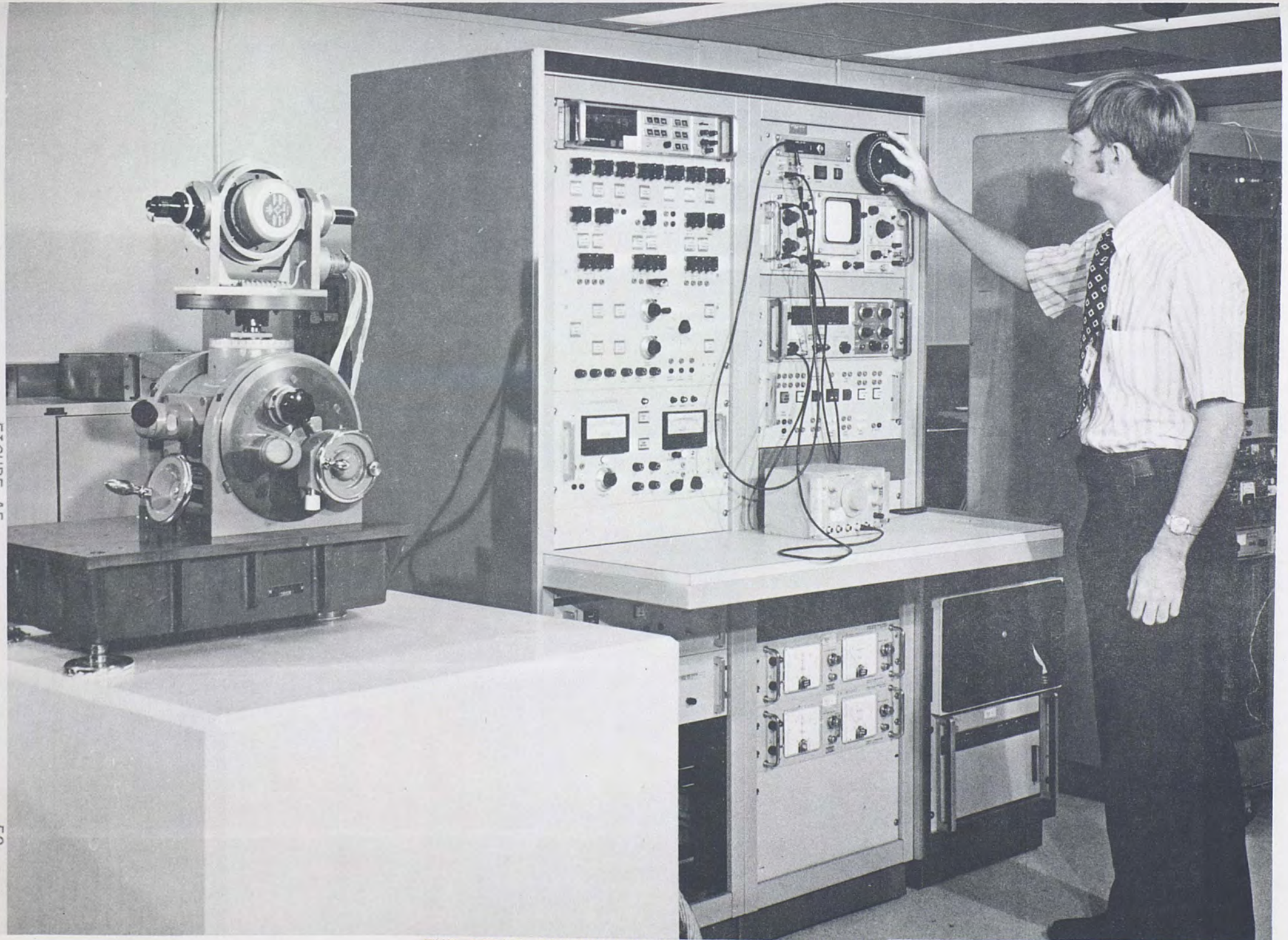

FIGURE A5

THE SERVO CONTROLLED FIXTURE IN OPERATION

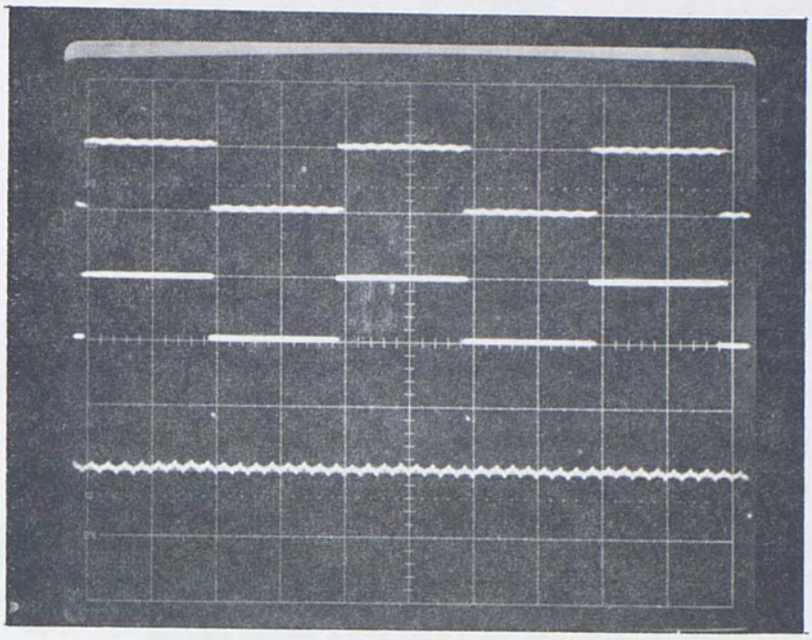

(a) 5°/SEC TURNTABLE RATE

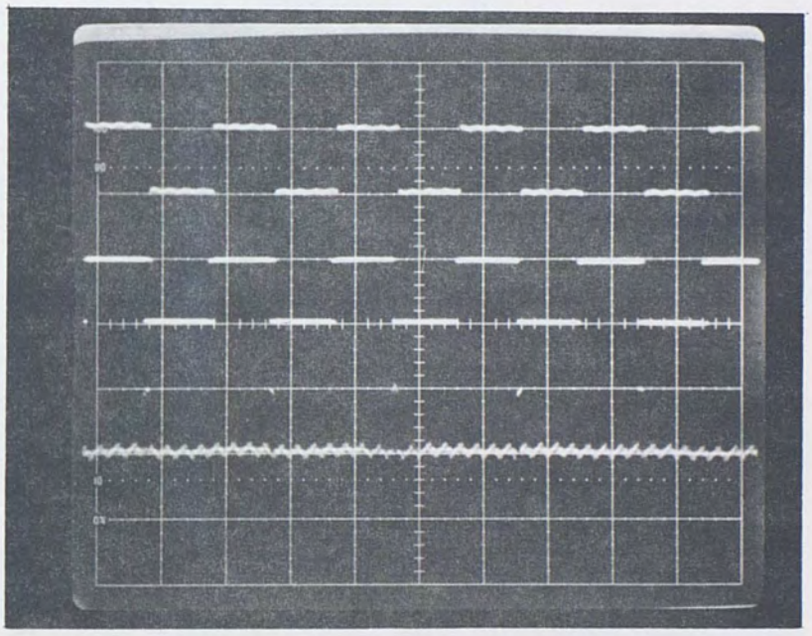

(b) 10°/SEC TURNTABLE RATE

FIGURE A6
THE PHASE DETECTOR OPERATION

CHANNEL 1: The Command Rate Frequency

CHANNEL 2: The Feed Back Rate Frequency

CHANNEL 3: The Phase Detector Error Pulses

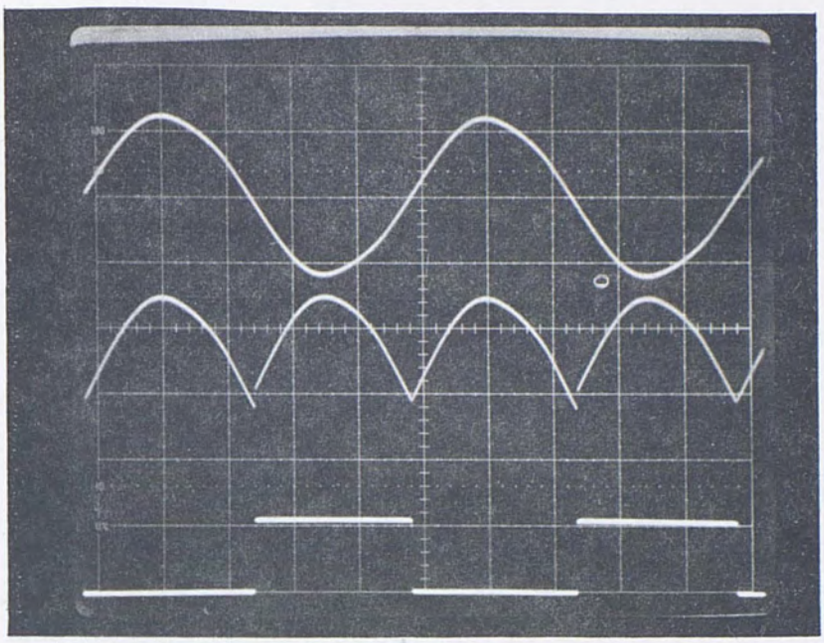

(a) 0° PHASED INPUT

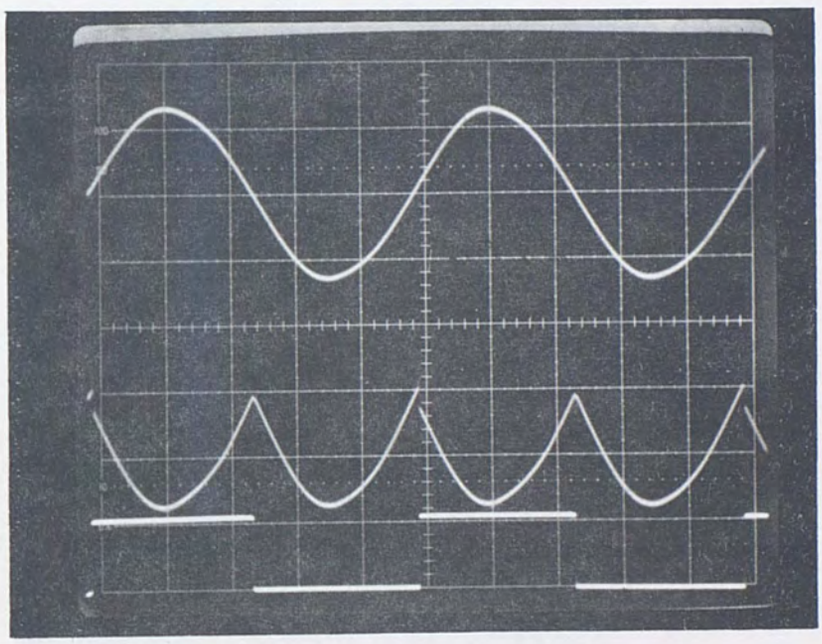

(b) 180° PHASED INPUT

FIGURE A7

THE POSITION LOOP SYNCHRONOUS DEMODULATOR OPERATION

CHANNEL 1: 400 Hz Resolver Information

CHANNEL 2: Demodulator Output

CHANNEL 3: Synchronous Square Wave for Gain Switching

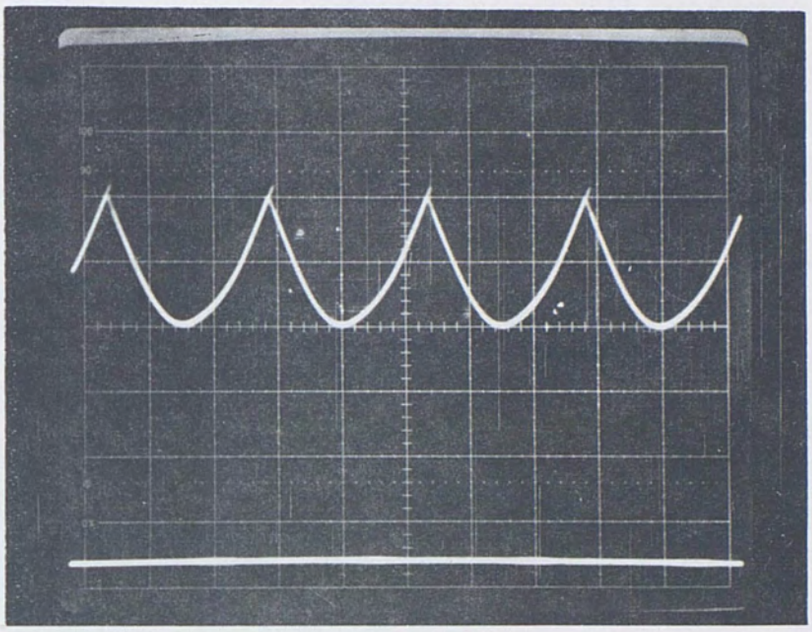

FIGURE A8

THE DEMODULATED POSITION INFORMATION
BEFORE AND AFTER FILTERING

CHANNEL 1: Demodulator Output

CHANNEL 2: 2ND Order Butterworth Filter Output

SELECTED BIBLIOGRAPHY

Glausi, Mohammed Shuaib. Principles and Design of Linear Active Circuits. New York: McGraw-Hill, Inc., 1965.

Kuo, Benjamin C. Automatic Control Systems. Englewood Cliffs, N. J.: Prentice-Hall, Inc., 1967.

Operational Amplifiers. New York: Burr Brown, 1971.